2-1-2014

An Abundant Dysfunctional Apolipoprotein A1 in Human Atheroma

Ying Huang
Cleveland Clinic

Joseph A. DiDonato
Cleveland State University, j.didonato41@csuohio.edu

Bruce S. Levison
Cleveland Clinic

Dave Schmitt
Cleveland Clinic

Lin Li
Cleveland Clinic

See next page for additional authors

Authors
Ying Huang, Joseph A. DiDonato, Bruce S. Levison, Dave Schmitt, Lin Li, Yuping Wu, Jennifer Buffa, Timothy Kim, Gary S. Gerstenecker, Xiaodong Gu, Chandra S. Kadiyala, Zeneng Wang, Miranda K. Culley, Jennie E. Hazen, Anthony J. DiDonato, Xiaoming Fu, Stela Z. Berisha, Daoquan Peng, Truc T. Nguyen, Shaohong Liang, Chia-Chi Chuang, Leslie Cho, Edward F. PLow, Paul L. Fox, Valentin Gogonea, W.H. Wilson Tang, John S. Parks, Edward A. Fisher, Jonathan D. Smith, and Stanley L. Hazen

An abundant dysfunctional apolipoprotein A1 in human atheroma

Ying Huang, Joseph A DiDonato, Bruce S Levison, Dave Schmitt, Lin Li Yuping Wu, Jennifer Buffa, Timothy Kim, Gary S Gerstenecker, Xiaodong Gu, Chandra S Kadiyala, Zeneng Wang, Miranda K Culley, Jennie E Hazen, Anthony J DiDonato, Xiaoming Fu, Stela Z Berisha, Daoquan Peng, Truc T Nguyen, Shaohong Liang, Chia-Chi Chuang, Leslie Cho, Edward F Plow, Paul L Fox, Valentin Gogonea, W H Wilson Tang, John S Parks, Edward A Fisher, Jonathan D Smith, Stanley L Hazen

Recent studies have indicated that high-density lipoproteins (HDLs) and their major structural protein, apolipoprotein A1 (apoA1), recovered from human atheroma are dysfunctional and are extensively oxidized by myeloperoxidase (MPO). *In vitro* oxidation of either apoA1 or HDL particles by MPO impairs their cholesterol acceptor function. Here, using phage display affinity maturation, we developed a high-affinity monoclonal antibody that specifically recognizes both apoA1 and HDL that have been modified by the MPO-H_2O_2-Cl^- system. An oxindolyl alanine (2-OH-Trp) moiety at Trp72 of apoA1 is the immunogenic epitope. Mutagenesis studies confirmed a critical role for apoA1 Trp72 in MPO-mediated inhibition of the ATP-binding cassette transporter A1 (ABCA1)-dependent cholesterol acceptor activity of apoA1 *in vitro* and *in vivo*. ApoA1 containing a 2-OH-Trp72 group (oxTrp72-apoA1) is in low abundance within the circulation but accounts for 20% of the apoA1 in atherosclerosis-laden arteries. OxTrp72-apoA1 recovered from human atheroma or plasma is lipid poor, virtually devoid of cholesterol acceptor activity and demonstrated both a potent proinflammatory activity on endothelial cells and an impaired HDL biogenesis activity *in vivo*. Elevated oxTrp72-apoA1 levels in subjects presenting to a cardiology clinic ($n = 627$) were associated with increased cardiovascular disease risk. Circulating oxTrp72-apoA1 levels may serve as a way to monitor a proatherogenic process in the artery wall.

HDL is a complex and heterogeneous assembly of proteins and lipids. Defined by its buoyant density isolation characteristics, HDL's compositional heterogeneity mirrors its functional heterogeneity, which includes cholesterol acceptor activity, microRNA delivery and anti-inflammatory, anti-apoptotic, anti-thrombotic and innate immune functions[1–6]. Approximately 75% of the protein content of HDL is apoA1, which serves as the primary protein scaffolding on which the lipid cargo-carrying particle is built. The majority of apoA1 within the circulation is associated with HDL particles, which contain two or more apoA1 polypeptide chains, depending on both the degree of particle maturation and the protein complement associated with a given HDL particle. Epidemiological studies have shown an inverse association between circulating HDL cholesterol (HDLc) or apoA1 levels and coronary artery disease (CAD)[7]. Animal studies using both genetic and direct infusion models have similarly shown global anti-atherosclerotic functions of the lipoprotein[8–12]. Recent clinical studies, however, have revealed gaps in our knowledge about HDL. For example, whereas several clinical intervention studies employing either direct infusion of HDL forms or infusion of extracorporeally delipidated HDL or apoA1 have shown anti-atherosclerotic effects[13–15], several distinct classes of HDL cholesterol–elevating drugs have, in contrast, failed to demonstrate significant therapeutic benefit[16–18]. Moreover, Mendelian genetic studies have demonstrated that genetic variants that influence total circulating HDLc levels are not mechanistically linked to the development of CAD[19]. Taken as a whole, recent studies underscore the complexity and evolving understanding of the relationship between circulating levels of HDLc and/or apoA1 and CAD pathogenesis.

One possible explanation of the paradox between, on the one hand, the well-established inverse association between HDLc levels and cardiovascular disease (CVD), and on the other, the negative outcomes of recent therapeutic intervention studies raising HDLc levels, is that it is HDL particle function, not HDLc mass, that is more clinically relevant diagnostically and therapeutically. For example, measurement of the cholesterol efflux activity of HDL, or of apoB-depleted serum, may serve as a superior independent predictor of prevalent CAD risk compared to HDLc[4]. Moreover, alternative functional measures of HDL or its associated proteins may provide improved clinical value and

prognostic efficacy[5,20–24]. Accordingly, current measures of HDL mass (either HDLc or apoA1) in the circulation do not appear to adequately reflect the pathobiology of a diseased artery wall. Recent studies of total apoA1 (both HDL-associated and lipid-poor forms) from human aortic tissues revealed that the biological function and HDL particle distribution of apoA1 within the artery wall are markedly distinct from those of circulating apoA1 and HDL. Specifically, apoA1 in human aorta was found to be predominantly lipid poor, not associated with HDL, extensively oxidatively crosslinked and functionally impaired[25]. ApoA1 serves as a selective target (100- to 500-fold relative to total protein) for oxidative modification by MPO-generated and nitric oxide–derived oxidants within the artery wall, resulting in site-specific oxidative modifications[26–28]. Parallel *in vitro* studies using HDL or apoA1 oxidized *ex vivo* by the MPO-H_2O_2-Cl^- system have shown marked reductions in their various activities—ABCA1-dependent cholesterol efflux function, lecithin cholesterol acyl transferase (LCAT) activity, lipid binding activity and non–cholesterol related activities (for example, anti-apoptotic and anti-inflammatory activities)—to an extent similar to that observed for apoA1 recovered from human lesions[26,28–30]. These findings, as well as studies demonstrating proinflammatory activities of HDL recovered from subjects with CAD or chronic inflammatory conditions associated with CAD risk[21,29,31–33], suggest that the molecular processes that impair apoA1 and HDL function in the artery wall may be diagnostic and therapeutic targets for CAD.

Here we report that Trp72 of apoA1 serves as a selective target for MPO-dependent oxidative modification, forming an oxindolyl alanine (2-hydroxy-L-tryptophan, or 2-OH-Trp; IUPAC name 2-amino-3-(2-oxo-1,3-dihydroindol-3-yl)propanoic acid) moiety on 20% of apoA1 recovered from human atherosclerotic lesions. We found that both lesion and plasma apoA1 harboring this site-specific modification were dysfunctional, with significantly impaired cholesterol efflux acceptor activity as well as proinflammatory effects. Moreover, data from clinical studies indicate that circulating levels of this dysfunctional apoA1 form reflect a pathophysiological process within the artery wall.

RESULTS

Development of an antibody specific for MPO-modified apoA1

Direct studies of HDL function in the human artery wall have been limited so far. To recover and study the chemical modifications and biological activities of HDL modified by MPO-generated oxidants in the artery wall, we developed immunological tools to specifically detect and immunopurify apoA1 modified by the MPO-H_2O_2-Cl^- system. We selected this specific oxidized form of apoA1 and HDL because *in vitro* studies have demonstrated that this system readily inhibits the cholesterol acceptor activity of both apoA1 and HDL under pathophysiologically plausible conditions[26,27,29]. After immunizing BALB/c mice with native reconstituted HDL particles (apoA1:POPC:cholesterol, 1:100:10, mol:mol:mol) exposed to either MPO-generated chlorinating oxidants (the MPO-H_2O_2-Cl^- system) or MPO-generated nitrating oxidants (the MPO-H_2O_2-NO_2^- system), we generated and screened over 30,000 hybridoma cell lines (**Supplementary Fig. 1a**). To ensure that the epitopes formed would be those likely to be formed under (patho)physiologically plausible conditions, we used a low molar ratio of H_2O_2 to apoA1 (5:1); under these conditions, the content of protein-bound 3-chlorotyrosine or 3-nitrotyrosine was within the range previously observed on apoA1 recovered from human atherosclerotic plaque[26,29]. We identified a monoclonal antibody (mAb) (clone 8B5.2) that specifically recognized both apoA1 and HDL exposed to the MPO-H_2O_2-Cl^- system but not apoA1 or HDL in their native (unoxidized) forms or after exposure to alternative oxidant systems, including the MPO-H_2O_2-NO_2^- oxidant system (**Supplementary Fig. 1a**).

Although mAb 8B5.2 had the desired specificity, its affinity was too low for either efficient immunoprecipitation or use in an ELISA format to detect endogenous circulating levels of oxTrp72-apoA1 (**Supplementary Fig. 1b–d**). We next used phage display technology to affinity mature (as a single-chain antibody) mAb 8B5.2 and then, after sequencing gain-of-function mutants, genetically engineered the recombinant IgG form (Online Methods). Briefly, we used human apoA1 exposed to the MPO-H_2O_2-Cl^- system as the positive-selection bait. After the first round of positive selection, we used as negative selection baits both native human apoA1 and human apoA1 exposed to MPO-generated nitrating oxidants (Online Methods). During the last two affinity maturation cycles, we sequenced multiple gain-of-function subclones and identified reproducible gain-of-function mutations. We then incorporated all gain-of-function mutants into a single clone and verified it to be functional as a high-affinity binder with the appropriate specificity. We then converted this 'combined' gain-of-function clone into a human-mouse chimeric IgG mAb (**Fig. 1a–c**). We termed this affinity-matured recombinant humanized mAb r8B5.2, which displayed a 1,600-fold enhanced affinity compared to the starting (parental) mAb, attaining a K_D of 1×10^{-10} M (**Supplementary Fig. 1c**). More detailed characterization studies confirmed that mAb r8B5.2 retained exclusive specificity for recognition of apoA1 exposed to the MPO-H_2O_2-halide system (**Fig. 1d**). Further characterization revealed that mAb r8B5.2 had sufficient affinity to immunoprecipitate MPO-oxidized apoA1 and, when used in an ELISA format, had adequate sensitivity to detect and quantify apoA1 and HDL after oxidation by the MPO-H_2O_2-Cl^- system at levels of oxidation comparable to those observed in plasma or serum (**Supplementary Fig. 1d**).

ApoA1 Trp72 oxidation inhibits cholesterol acceptor function

No studies to our knowledge have directly examined the functional importance of modification of apoA1 or HDL by MPO within human atheroma. Rather, the proposed *in vivo* effect of MPO-catalyzed oxidation of apoA1 and HDL—impairing the cholesterol acceptor activity of the lipoprotein—is based on correlative data that compare the degree of oxidative modifications on apoA1 recovered from artery wall tissues with both the extent of oxidative modifications formed and the degree of ABCA1-dependent cholesterol efflux impairment observed in model systems *ex vivo*[26,29]. Incubation of apoA1 or HDL with the MPO-H_2O_2-Cl^- system can promote oxidative modification of multiple oxidant-sensitive residues of apoA1, including (but not limited to) each of the three methionines, each of the seven tyrosines and each of the four tryptophans. Oxidation of each of these residues has been detected by proteomics analysis of apoA1 or HDL recovered from human atherosclerotic lesions, yet debate exists about the relative abundance of various species and their functional importance[26–29,34]. We hypothesized that the epitope recognized by mAb r8B5.2 might be an oxidized form of tyrosine, methionine or tryptophan generated by the MPO-H_2O_2-Cl^- system within the appropriate sequence context of apoA1. To test this idea, we generated recombinant mutant forms of apoA1 in which each of these residues was converted to a relatively nonoxidizable alternative amino acid of similar size and chemical properties, namely (i) each of the seven tyrosine residues (positions 18, 29, 100, 115, 166, 192 and 236) was mutated to the relatively nonoxidizable phenylalanine

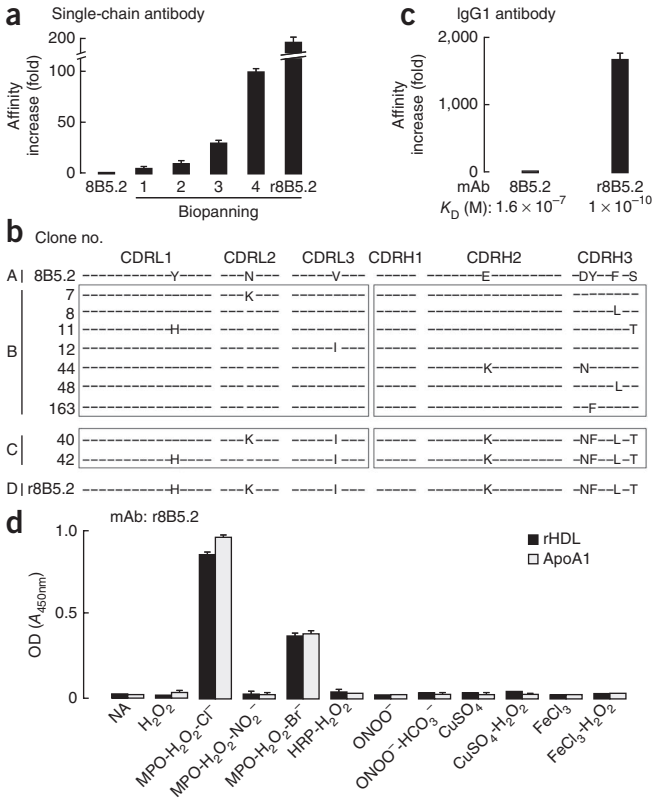

Figure 1 Phage display affinity maturation to form a high-affinity mAb specific for apoA1 oxidized by the MPO-H_2O_2-halide system. (**a**) Fold increase in apparent binding affinity after the indicated rounds (1–4) of biopanning after phage display affinity maturation of the parental mouse mAb 8B5.2 single-chain antibody (scFv). r8B5.2, the recombinant affinity matured scFv antibody. (**b**) Complementarity-determining region (CDR) DNA sequences of the original mAb 8B5.2 and those of nine affinity-matured scFv r8B5.2 subclones identified with lowest dissociation rate. CDRL1-3, CDRs of antibody light chain; CDRH1-3, CDRs of antibody heavy chain. The letters indicate the identities of the mutated amino acids and the differences between original and affinity-matured clones. (**c**) The increase in apparent affinity (K_D) of the parental mAb 8B5.2 antibody and the affinity-matured scFv r8B5.2 antibody after conversion to a full-length mouse-human chimeric IgG1, designated as r8B5.2. (**d**) ApoA1 or reconstituted HDL (rHDL) in native form, or following exposure to the indicated oxidation systems, were coated onto 96-well plates and detected with r8B5.2 (Online Methods). OD, optical density; A_{450nm}, absorbance at 450 nm; NA, no addition. All data are shown as the mean ± s.d. of triplicate determinations.

residue (a mutant named 7YF); (ii) each of the three methionine residues (positions 86, 112 and 148) was mutated to the relatively nonoxidizable valine residue (a mutant named 3MV); and (iii) each of the four tryptophan residues (positions 8, 50, 72 and 108) was mutated to the relatively nonoxidizable phenylalanine residue (a mutant named 4WF). We reasoned that after exposure of the lipoprotein to the MPO-H_2O_2-Cl^- system, the mutant form of apoA1 no longer harboring the oxidant-sensitive residue would not be recognized by mAb r8B5.2, whereas recombinant human (wild-type sequence) apoA1 (rh-apoA1) would be recognized after oxidation. Exposure of rh-apoA1, 7YF and 3MV to the MPO-H_2O_2-Cl^- system produced an oxidized apolipoprotein that was recognized by mAb r8B5.2, whereas the apoA1 mutant 4WF was not recognized after oxidation (**Fig. 2a**). Notably, control studies showed that all mutant forms of apoA1 examined retained cholesterol efflux activity in their native forms, and all forms but 4WF lost ABCA1-dependent and total cholesterol efflux activities after exposure to the MPO-H_2O_2-Cl^- system (**Fig. 2b**). Collectively, these results suggest that one or more of the tryptophan residues of apoA1 contribute to formation of the epitope recognized by mAb r8B5.2 after oxidation by the MPO-H_2O_2-Cl^- system. Moreover, these data indicate that one or more of the tryptophan residues functions as an oxidative switch for impairing the cholesterol efflux activity of apoA1.

To identify the oxidized tryptophan residue that serves as the epitope recognized by mAb r8B5.2, we generated additional site-specific mutant forms of apoA1 in which each of the four tryptophan residues was converted singly to leucine (W8L, W50L, W72L and W108L). Alternatively, each of two of the residues was converted singly to phenylalanine (W72F and W108F). The MPO-oxidized form of each recombinant apoA1 mutant was recognized by the antibody except for mutants with site-specific mutation of Trp72 (**Fig. 2a**). Competition experiments using a molar excess of different oxidized forms of tryptophan (as free amino acids) suggested that the oxygen at the 2 position of the indole ring was important for epitope recognition (**Supplementary Fig. 2**). We confirmed that a 2-oxindolyl alanine, the 2-OH-Trp moiety at Trp72 of apoA1 (oxTrp72-apoA1), is the recognition site for mAb r8B5.2 using two additional ELISA-based competition experiments. In the first experiment, we used synthetic peptides containing the sequences in apoA1 that span each of the four tryptophan residues, in which the peptide was either in its native form (with a Trp residue) or in its oxidized form (with a 2-OH-Trp residue) (**Fig. 2c**). In the second experiment, we used a peptide spanning Trp72 in which Trp within the peptide was in its native form or in its 2-OH or 5-OH indole–oxidized forms (**Fig. 2d**).

We next sought to determine the functional importance of Trp72 for the cholesterol acceptor activity of apoA1 in native and MPO-oxidized conditions. Exposure of native recombinant human apoA1 to increasing levels of oxidation by the MPO-H_2O_2-Cl^- system at molar ratios of H_2O_2 to apoA1 of ~0–2 resulted in little loss of ABCA1-dependent cholesterol efflux activity (**Fig. 2e**). Mass spectrometry studies detected methionine sulfoxide formation at each of the three apoA1 methionine residues at these low levels of oxidation (data not shown). However, with increasing molar ratios of H_2O_2 to apoA1, there was an abrupt dose-dependent inhibition of ABCA1-dependent cholesterol acceptor activity, with virtually no remaining activity at a 10:1 molar ratio (**Fig. 2e**). This level of oxidant exposure is within the upper end of that observed within atherosclerotic plaques, based on the protein-bound 3-chlorotyrosine content of apoA1, as monitored by liquid chromatography tandem mass spectrometry (LC/MS/MS) analyses (**Supplementary Fig. 1d**). In contrast, the 4WF apoA1 mutant was resistant to oxidative inactivation of ABCA1-dependent cholesterol acceptor activity, with unaltered activity even in the presence of a 50-fold molar excess of oxidant relative to apoA1 (**Fig. 2e**), a result that is consistent with previous reports[28]. We next examined the effect of site-specific mutation of Trp72 to a relatively oxidant-resistant hydrophobic residue (phenylalanine or alanine). Either mutation resulted in an approximate 50% reduction in ABCA1-dependent cholesterol efflux activity at a tenfold molar excess of oxidant (**Fig. 2e**). Alternatively, apoA1 in which the other three tryptophan residues of apoA1 were mutated to phenylalanine (the 3F72W mutant) showed a similar extent (~50%) of functional inactivation under the same oxidant conditions (**Fig. 2e** and **Supplementary Fig. 1d**). Collectively these studies indicate that after exposure to the MPO-H_2O_2-halide system, oxidation of Trp72 of apoA1, yielding a

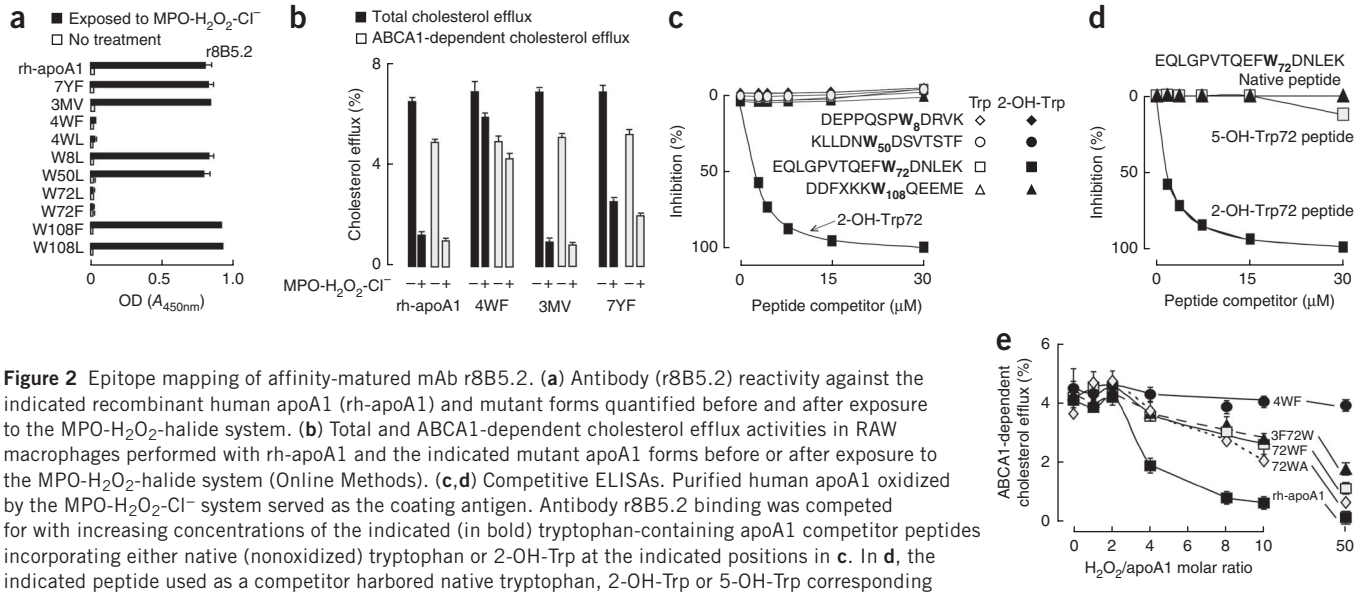

Figure 2 Epitope mapping of affinity-matured mAb r8B5.2. (**a**) Antibody (r8B5.2) reactivity against the indicated recombinant human apoA1 (rh-apoA1) and mutant forms quantified before and after exposure to the MPO-H_2O_2-halide system. (**b**) Total and ABCA1-dependent cholesterol efflux activities in RAW macrophages performed with rh-apoA1 and the indicated mutant apoA1 forms before or after exposure to the MPO-H_2O_2-halide system (Online Methods). (**c**,**d**) Competitive ELISAs. Purified human apoA1 oxidized by the MPO-H_2O_2-Cl^- system served as the coating antigen. Antibody r8B5.2 binding was competed for with increasing concentrations of the indicated (in bold) tryptophan-containing apoA1 competitor peptides incorporating either native (nonoxidized) tryptophan or 2-OH-Trp at the indicated positions in **c**. In **d**, the indicated peptide used as a competitor harbored native tryptophan, 2-OH-Trp or 5-OH-Trp corresponding to position 72. (**e**) Effect of tryptophan substitutions on rh-apoA1 ABCA1-dependent cellular cholesterol efflux function. The indicated rh-apoA1 and mutant apoA1 proteins were exposed to the MPO-H_2O_2-Cl^- oxidation system at the specified molar ratios of H_2O_2 to apoA1 (0 to 50:1, mol:mol). Proteins were assayed for ABCA1-dependent cellular cholesterol acceptor activity (Online Methods). All data shown are the means ± s.d. of at least triplicate determinations.

2-oxindolyl alanine (2-OH-Trp) moiety, is specifically recognized by mAb r8B5.2 (henceforth we refer to apoA1 detected by mAb r8B5.2 as oxTrp72-apoA1 to indicate the epitope recognized). Moreover, oxidation of this residue is responsible for about 50% of the the loss of cholesterol acceptor function of the oxidized lipoprotein.

Lesion apoA1 harbors a 2-OH-Trp72 group and is dysfunctional

Using this new immunological tool, we found by immunohistochemical staining that oxTrp72-apoA1 is present in human atherosclerotic plaques but not in normal human aorta (**Fig. 3a**). Staining of arterial tissues in parallel with an antibody to MPO revealed a staining pattern within plaques that was similar overall to that observed with anti–oxTrp72-apoA1. However, whereas oxTrp72-apoA1 was not detectable in normal arterial tissue, we did detect weak MPO staining in this tissue, with staining along the endothelial surface, within endothelial cells and in the narrow subendothelial space (**Supplementary Fig. 3a,b**). To further characterize oxTrp72-apoA1 in human aortic plaque, we performed an SDS-PAGE analysis of human aortic plaque homogenate ($n = 5$ subjects). For this analysis, we used the low-speed supernatant of the homogenate either before or after buoyant density ultracentrifugation to separate a global lipoprotein fraction (density (d) ≤ 1.21 g ml^{-1}) from the lipoprotein-depleted (LPD) fraction (d > 1.21 g ml^{-1}) (**Fig. 3b**). Western blot analyses performed in parallel using mAb r8B5.2 revealed that virtually all detectable oxTrp72-apoA1 resided in a lipid-poor soluble form (i.e., a form that was not lipoprotein associated) (**Fig. 3c**). More detailed quantification showed that ~80% of oxTrp72-apoA1 within human aortic plaque homogenate was recovered in the LPD fraction and <1% was recovered within the lipoprotein-containing fraction (**Fig. 3d**).

We next studied the functional characteristics of oxTrp72-apoA1 recovered from human atherosclerotic plaques. We used an affinity column with covalently linked mAb r8B5.2 to isolate an apoA1 form harboring the 2-OH-Trp moiety at residue 72 (oxTrp72-apoA1) from human artery lesion homogenates. Affinity-isolated oxTrp72-apoA1 analyzed by SDS-PAGE appeared to be at high purity: the major visible bands were at the molecular weights anticipated for the apoA1 monomer and dimer (**Fig. 3e**). Mass spectrometry analyses directly detected tryptic peptides containing oxTrp72 (OH) (**Supplementary Fig. 3c**), and virtually no tryptic peptides harboring native (unoxidized) Trp72 were recovered. Furthermore, mass spectrometry analyses of excised bands corresponding to the presumed monomer, dimer, trimer and higher–molecular weight crosslinked forms of apoA1 revealed that they all predominantly contained apoA1 (**Supplementary Table 1a**,**b**). We next examined the cholesterol acceptor function of oxTrp72-apoA1 recovered from aortic lesions from multiple subjects ($n = 6$). Even at a concentration (10 μg ml^{-1}) that was twice that used for native human apoA1 (used as the positive control), oxTrp72-apoA1 used as a cholesterol acceptor showed only negligible ABCA1-dependent cholesterol efflux activity (**Fig. 3f**). Collectively, these results demonstrate that oxTrp72-apoA1, an MPO-modified form of apoA1 present within human atheroma, is predominantly non-HDL (lipoprotein) associated and is dysfunctional with respect to cholesterol efflux activity.

Plasma oxTrp72-apoA1 is proinflammatory

To examine the distribution of oxTrp72-apoA1 in the circulation, we fractionated plasma from multiple healthy subjects (six pooled healthy donor pools, each pool was obtained from ≥ five subjects) by buoyant density ultracentrifugation and determined the level of oxTrp72-apoA1 within each fraction. Similarly to human atherosclerotic plaques, virtually all detectable oxTrp72-apoA1 in the plasma resided in the LPD fraction (d > 1.21 g ml^{-1}), with only nominal levels recovered in the HDL fraction (d = 1.063–1.21 g ml^{-1}) (**Fig. 4a–c**). Because of the possibility that the high shear forces of ultracentrifugation might 'knock off' oxTrp72-apoA1 from the HDL, we performed additional studies to verify these findings. Using polyclonal antibodies (anti-HDL IgY) raised in chickens against human HDL (isolated from plasma of healthy volunteers) and covalently attached to resin, we immunoisolated HDL from the plasma of ten healthy (>50 years of age) subjects with no known CAD. Separate studies of the binding characteristics of the anti-HDL IgY antibody revealed preferential

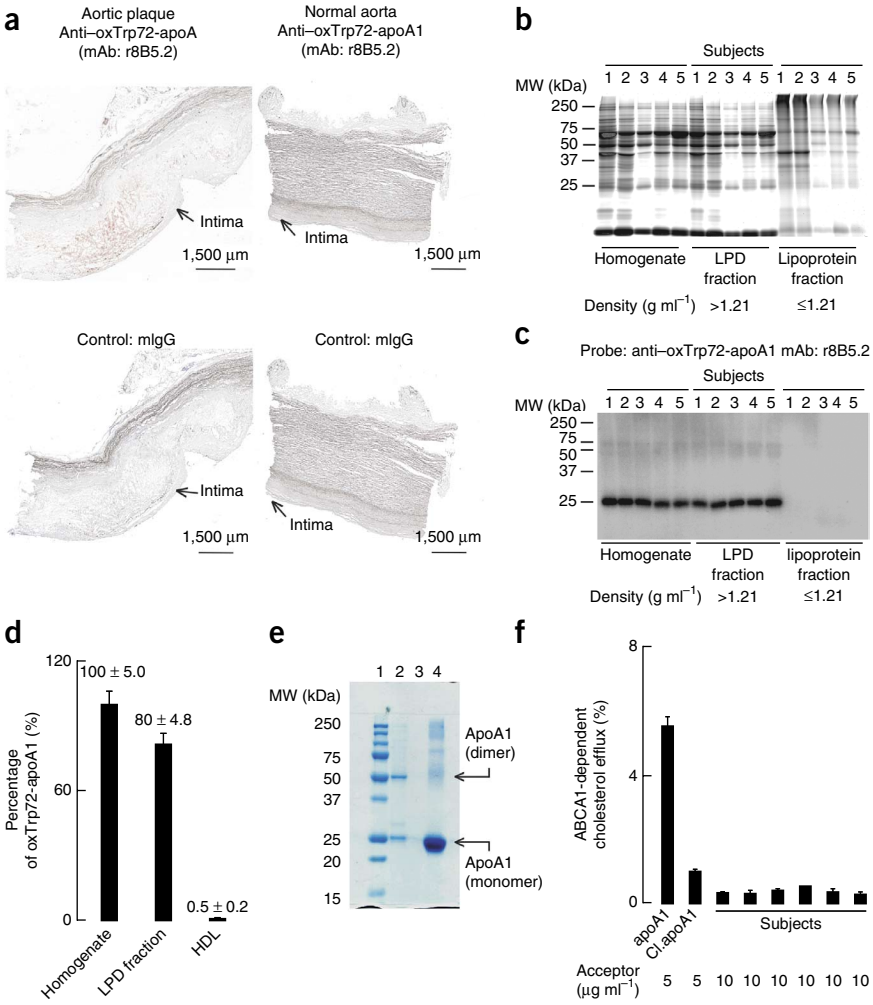

Figure 3 Characterization of oxTrp72-apoA1 recovered from human atherosclerotic plaque. (**a**) Immunohistochemical staining of fresh-frozen normal and atherosclerotic sections of human aorta. OxTrp72-apoA1 was detected with mAb r8B5.2. Mouse IgG was used as the control. Red, positive staining; blue, H&E counter stain. (**b**,**c**) SDS-PAGE, protein (SYPRO ruby) staining (**b**) and western blot analysis (**c**) of human aortic plaque homogenate and the indicated fractions separated by buoyant density ultracentrifugation. (**d**) OxTrp72-apoA1 levels (as a percentage of total apoA1) recovered in human atherosclerotic tissue homogenate and in the lipoprotein ($d \leq 1.21$ g ml^{-1}) and LPD ($d > 1.21$ g ml^{-1}) fractions. The data are shown as the means ± s.d. of triplicate determinations of $n = 4$ subjects. (**e**) SDS-PAGE followed by Coomassie Blue (protein) staining of mAb r8B5.2–immunopurified oxTrp72-apoA1 from human aortic tissue (lane 2). As a positive control, apoA1 exposed to the MPO-H_2O_2-Cl^- system (at a 10:1 molar ratio of H_2O_2 to apoA1; Cl.apoA1), was loaded in lane 4. The ApoA1 monomer and dimer are indicated. MW, molecular weight markers (lane 1); IP, immunoprecipitation. Lane 3 is empty. (**f**) ABCA1-dependent cholesterol efflux activity of oxTrp72-apoA1 immunoaffinity purified from individual ($n = 6$ subjects) human aortic plaques. Each bar represents data from a different subject's sample. Native apoA1 and Cl.apoA1 were used as controls. Results shown are mean ± s.d. of triplicate determinations.

recognition of lipidated (HDL-associated) apoA1 but also clear recognition of lipid-free apoA1 (data not shown). Recovery of HDL from the plasma of each subject was confirmed by Coomassie Blue staining of native gels (**Supplementary Fig. 4a**). Western blot analyses with mAb 10G1.5 (termed anti-total apoA1), which recognizes equally well native and oxidized forms of apoA1 and HDL[25], confirmed the presence of apoA1 within the immunoaffinity-isolated material from each subject (**Supplementary Fig. 4b**). In contrast, western blot analyses of native gels using mAb r8B5.2 failed to detect any bands within the HDL fractions even with extensive overexposure (**Supplementary Fig. 4c**). However, mAb r8B5.2 did detect bands if used in western blot analyses of the samples using SDS-PAGE and with extensive overexposure (data not shown). Together, these results indicate that oxTrp72-apoA1, although present within the circulation, does not reside on an HDL particle to any major extent, but rather is present as a low-abundance lipid-poor form of apoA1 in the LPD fraction.

We next used mAb 8B5.2 to immunoaffinity isolate circulating oxTrp72-apoA1 from healthy subjects (multiple healthy donor pools, each pool was obtained from ≥ five subjects) to characterize its biological activity. By Coomassie Blue staining, the recovered protein appeared to be of high purity, with the major visible bands corresponding to the apoA1 monomer and oxidative crosslinked dimer (**Fig. 4d**). By mass spectrometry analyses the recovered bands were confirmed to be apoA1, with multiple peptides containing oxidized residues (predominantly tryptophan and methionine; **Supplementary Table 1c**). Western blot analyses of the immunopurified apoA1 performed in parallel showed bands at the anticipated molecular weights of the apoA1 monomer and dimer using mAb r8B5.2 or mAb 10G1.5 (**Supplementary Fig. 4d**). No detectable light or heavy chain immunoglobulin contamination was observed under the conditions employed (**Supplementary Fig. 4d**).

We and others have shown that HDL isolated from healthy volunteers has anti-inflammatory effects when incubated with bovine aortic endothelial cells, whereas apoA1 or HDL modified by MPO *ex vivo* converts the lipoprotein into a proinflammatory particle[29]. We therefore examined the proinflammatory properties of oxTrp72-apoA1 recovered from the circulation of a nonoverlapping set of apparently healthy middle aged (>50 years of age) donors ($n = 12$). For comparison, we isolated total apoA1 from the same donors using polyclonal chicken IgY antibodies raised against native human apoA1 (**Fig. 4e**). After incubation of oxTrp72-apoA1 recovered from each subject's plasma with bovine aortic endothelial cells, we observed a marked proinflammatory effect, as monitored by substantial increases in surface vascular cell adhesion molecule 1 (VCAM1) protein content. In contrast, apoA1 recovered from plasma using immunoprecipitation with the anti-HDL IgY antibodies, or a comparable amount of total plasma protein, did not elicit a proinflammatory response in the endothelial cells (**Fig. 4e**). Moreover, immuno-isolated lipid-free (i.e., after organic solvent extraction) oxTrp72-apoA1 recovered from plasma promoted endothelial cell nuclear factor-κB (NF-κB) activation and nuclear localization, similarly to *in vitro*–oxidized lipid-free apoA1 (using the MPO-H_2O_2-Cl^- system) or interleukin-1 (IL-1), used as positive controls. In contrast to lipid-free oxTrp72-apoA1, lipid-free

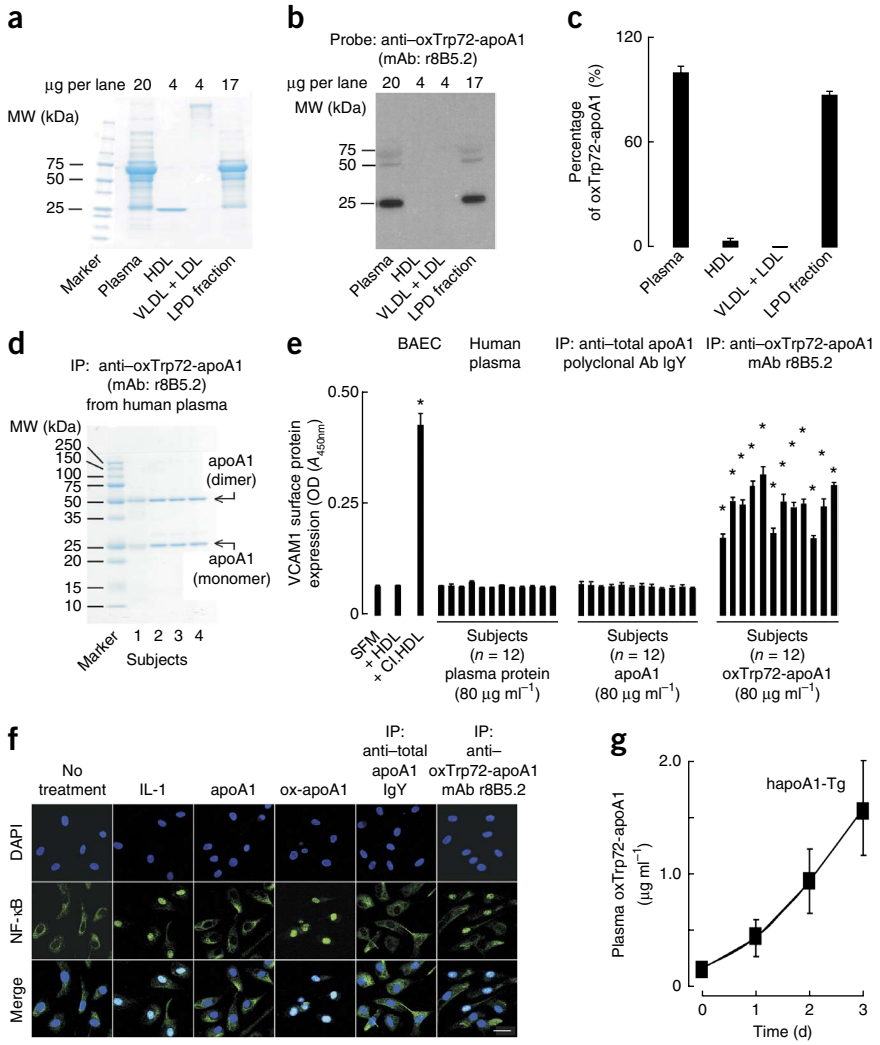

Figure 4 Characterization of oxTrp72-apoA1 recovered from human plasma. (**a**,**b**) SDS-PAGE followed by Coomassie Blue staining (**a**) or western blot for detection of oxTrp72-apoA1 (using mAb 8B5.2) (**b**) of human plasma proteins before and after buoyant density ultracentrifugation separation into the indicated fractions. (**c**) Distribution of oxTrp72-apoA1 in the plasma. Results shown are the mean ± s.d. of triplicate determinations of six pooled healthy donor plasma pools (each pool was obtained from at least $n = 5$ subjects). (**d**) SDS-PAGE followed by Coomassie Blue staining of immunopurified (using mAb r8B5.2) oxTrp72-apoA1 from plasma from four donors. (**e**) Surface VCAM1 protein expression quantified by cell-based ELISA (Online Methods) of bovine aortic endothelial cells (BAEC) incubated with plasma protein, total apoA1 (recovered from plasma using immobilized anti–total apoA1 IgY) or oxTrp72-apoA1 (recovered from plasma using immobilized mAb r8B5.2) from 12 individual subjects. Serum-free media (SFM), HDL or HDL previously exposed to the MPO-H_2O_2-Cl^- system (Cl.HDL, at H_2O_2:apoA1, 10:1, mol:mol) were used as the vehicle, negative and positive controls, respectively. $^*P < 0.05$. Results shown are mean ± s.d. of triplicate determinations, and P values represent comparisons between subject samples versus SFM and were determined using the Wilcoxon and Kruskal-Wallis tests. (**f**) Nuclear translocation of NF-κB was assessed by confocal immunofluorescent analysis of BAECs, which were untreated or treated with the following: IL-1 (positive control), native apoA1 (apoA1), MPO-oxidized human apoA1 (ox-apoA1), plasma-derived total apoA1 immunopurified using IgY to apoA1 or plasma oxTrp72-apoA1 immunopurified using r8B5.2. NF-κB p65 (Glu498) staining is green and nuclear counterstaining (DAPI) is blue. (**g**) Plasma oxTrp72-apoA1 levels were quantified at the indicated times in human apoA1 transgenic (hapoA1-Tg) mice injected i.p. with zymosan ($t = 0$). Quantification was performed by sandwich ELISA using mAb r8B5.2 as the capture antibody and mAb 10G1.5 (anti–total apoA1) as the detection antibody (Online Methods). Results shown are mean ± s.d. of triplicate determinations from $n = 3$ animals.

native apoA1 isolated from plasma HDL recovered from healthy volunteers did not induce NF-κB activation (**Fig. 4f**).

We next investigated whether formation of oxTrp72-apoA1 is specific to atherosclerotic plaque or if it occurs in other subacute inflammatory conditions, such as in a peritonitis model, in which inflammation is induced by the intraperitoneal (i.p.) injection of yeast cell-wall protein carbohydrate components (zymosan). We have previously shown that MPO serves as a major enzymatic catalyst for both protein and lipid oxidation in this model[35]. In human apoA1 transgenic mice, formation of oxTrp72-apoA1 was readily detectable over time in both peritoneal lavage fluid (data not shown) and plasma, demonstrating that endogenous human apoA1 is targeted for post-translational modification at Trp72 during subacute inflammation (**Fig. 4g**). Thus, apoA1 may be oxidized at a local site of inflammation, such as an atherosclerosis-laden artery wall or an inflamed peritoneal cavity, and then diffuse into the circulation.

OxTrp72-apoA1 has impaired HDL biogenesis activity *in vivo*

ABCA1 is critical for HDL biogenesis, and hepatocyte ABCA1 expression accounts for nearly 80% of plasma HDL production[36]. Given that MPO potently inhibits the ABCA1-dependent cholesterol efflux activity of apoA1 and HDL *in vitro*, and that our site-directed mutagenesis studies support a crucial role for apoA1 Trp72 in ABCA1-dependent efflux activity (**Fig. 2e**), we wanted to test whether oxTrp72-apoA1 recovered from human plasma has an impaired capacity to stimulate HDL biogenesis *in vivo*. We first sought to develop an animal model that would allow us to monitor ABCA1-dependent nascent HDL particle formation *in vivo*. We found that injection of lipid-free human apoA1 subcutaneously (s.c.) into apoA1 knockout (KO) mice resulted in the appearance of apoA1 in the vascular compartment (i.e., plasma), time-dependent increases in circulating HDL particle cholesterol content and incorporation of human apoA1 into the HDL particle pool (**Fig. 5a–d**). To determine whether these were ABCA1-dependent phenomena, we injected lipid-free human apoA1 s.c. into hepatocyte-specific ABCA1 KO mice and the appropriate ABCA1 floxed controls[36]. In contrast to ABCA1 floxed control mice, where time-dependent increases in HDLc were noted and virtually all circulating apoA1 was HDL-associated, injection of apoA1 into ABCA1 KO mice did not result in a time-dependent increase in plasma HDLc levels (**Supplementary Fig. 5a–c**).

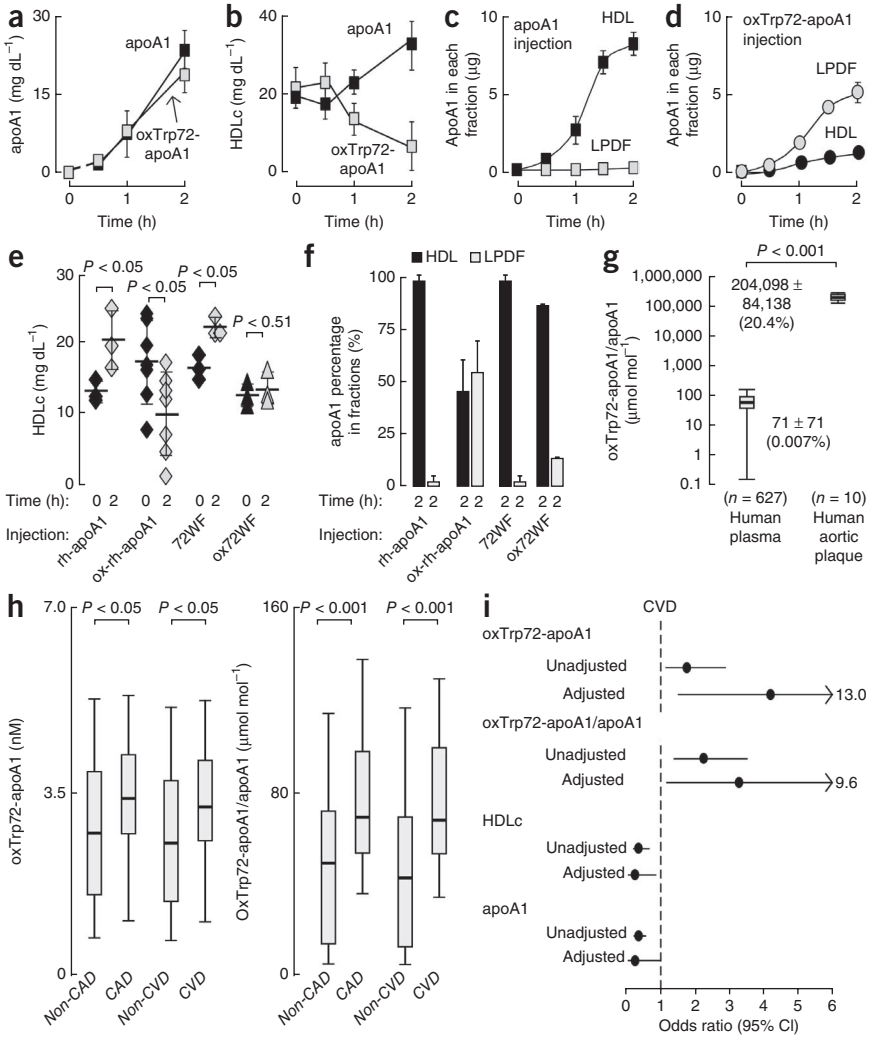

Figure 5 oxTrp72-apoA1 has impaired function in vivo and is associated with CVD. (**a**–**d**) Total apoA1 levels (**a**), HDLc levels (**b**) and apoA1 distribution within the HDL and lipoprotein-depleted fractions (LPDF) of plasma (**c**,**d**) quantified at the indicated times in apoA1 KO mice (6–8 weeks old) injected s.c. with equivalent amounts of apoA1 or oxTrp72-apoA1 (Online Methods). Data shown are mean ± s.d. (**a**,**b**) and mean ± s.e.m. (**c**,**d**) of triplicate determinations of $n = 3$ mice in each group. (**e**) Plasma HDLc levels in apoA1 KO mice injected s.c. with equivalent amounts of rh-apoA1, 72WF or their corresponding MPO-oxidized forms (formed at H2O2:apoA1, 10:1, mol:mol). Plasma HDLc levels were determined before and 2 h after apoA1 injections. Each symbol shown represents an individual mouse. (**f**) apoA1 distribution in plasma between the HDL ($d = 1.063$–1.21 g ml^{-1}) and LPD ($d \geq 1.21$ g ml^{-1}) fractions expressed as a percentage of the total apoA1 in plasma 2 h after apoA1 injection. Data shown are mean ± s.d. of triplicate determinations of $n = 3$ mice in each group. (**g**) Levels of oxTrp72-apoA1 (relative to total apoA1) in plasma and human aortic plaque homogenate from the indicated number of subjects. Levels were quantified by sandwich ELISA using mAb r8B5.2 as the capture antibody and mAb 10G1.5 (anti–total apoA1) as the detection antibody. Wilcoxon and Kruskal-Wallis tests were used to calculate P values. The value shown (bar) is the mean ± s.d. (**h**) Box-and-whisker plots of oxTrp72-apoA1 concentration and the ratio of oxTrp72-apoA1 to total apoA1 (as a percentage) within the plasma among subjects ($n = 627$) within the cohort stratified by the presence versus absence of either CAD or CVD as indicated. The box-and-whisker plots show percentiles (10%, 25%, 50%, 75% and 90%). Wilcoxon and Kruskal-Wallis tests were used to calculate P values. (**i**) Odds ratio (symbols) and 95% confidence intervals (CI; line or arrow) for CVD risk (unadjusted and after multilogistic regression analyses). The fully loaded model included oxTrp72-apoA1, apoA1, age, sex, hypertension, diabetes, smoking, HDLc, circulating low-density lipoprotein (LDLc), triglycerides, high-sensitivity C-reactive protein, hemoglobin A1C (HgbA1c), MPO and lipid lowering medicine.

Moreover, in ABCA1 KO mice, virtually no human apoA1 appeared within the HDL fraction (**Supplementary Fig. 5a–c**).

Using this *in vivo* model of ABCA1-dependent HDL biogenesis, we next tested whether oxTrp72-apoA1 recovered from human plasma was indeed dysfunctional *in vivo*. Injection of apoA1 KO mice s.c. with equivalent amounts of either lipid-free native human apoA1 or immunoaffinity-isolated oxTrp72-apoA1 resulted in comparable time-dependent appearances of total apoA1 in the circulation (**Fig. 5a**). However, whereas s.c. injection of native human apoA1 induced time-dependent increases in HDLc levels over a short period of time (2 h), injection of oxTrp72-apoA1 did not increase HDLc levels (despite being present in the vascular compartment), and reproducibly even slightly reduced HDLc levels (**Fig. 5b**). Native human apoA1 appearing in the circulation resided entirely within HDL particles (**Fig. 5c**), whereas oxTrp72-apoA1 remained predominantly within the LPD fraction (**Fig. 5d**). Thus, oxTrp72-apoA1 recovered from human plasma is deficient in ABCA1-dependent HDL biogenesis activity *in vivo*.

We next tested whether an apoA1 form in which Trp72 is mutated to phenylalanine (72WF-apoA1), which is resistant to MPO-catalyzed oxidative inactivation *in vitro* (**Fig. 2e**), demonstrates improved biological function relative to native human apoA1 after oxidation. We examined native wild-type recombinant human apoA1 (rh-apoA1) and 72WF-apoA1 for *in vivo* HDL biogenesis activity in both their native and MPO-oxidized forms. After s.c. injection of either the native or oxidized forms of rh-apoA1 or 72WF-apoA1 into apoA1 KO mice, comparable total plasma apoA1 levels were observed (**Supplementary Fig. 6a**). Within 2 h after injection of native rh-apoA1, we observed time-dependent increases in plasma HDLc levels, consistent with *de novo* HDL biogenesis (**Fig. 5e**). In contrast, injection of rh-apoA1 exposed to the MPO-H_2O_2-Cl^- system (apoA1:H_2O_2, 10:1) led to a time-dependent decrease (within 2 h) in HDLc levels (**Fig. 5e**). Injection of native 72WF-apoA1 led to a similar increase in HDLc levels compared to native rh-apoA1, but injection of oxidized 72WF-apoA1 did not lead to a reduction in HDLc levels (**Fig. 5e**). More substantial differences between the behavior of rh-apoA1 and 72WF-apoA1 were revealed by examination of the HDL particle distribution of the injected apoA1 (**Fig. 5f** and **Supplementary Fig. 6b**). Whereas most of the injected oxidized rh-apoA1 failed to become incorporated into HDL particles, virtually all of the injected oxidized 72WF-apoA1

did so (**Fig. 5f**). Thus, site-specific mutation of Trp72 into the oxidant-resistant residue phenylalanine produced a mutant form of apoA1 that was protected from oxidative loss of HDL biogenesis activity, consistent with *in vitro* data demonstrating an improved interaction with ABCA1 (**Fig. 2e**).

OxTrp72-apoA1 is abundant in human atheroma and predicts CVD

To quantify the content of oxTrp72-apoA1 in human plasma and aortic atherosclerotic plaque homogenate, we developed a sandwich immunoassay. In this assay, mAb r8B5.2 was used as the capture antibody, and mAb 10G1.5 was used as the detection antibody (mAb 10G1.5 recognizes native and oxidized forms of apoA1 and HDL to comparable extents, and also recognizes lipid-free and HDL-associated apoA1 to comparable extents). We examined sequential consenting subjects (n = 627) undergoing elective risk-factor evaluation and cardiac examination in an outpatient preventive cardiology clinic. Examination of the clinical and demographic characteristics of the cohort (**Supplementary Table 2a**) showed that 35% of subjects had clinical evidence of CVD. Quantification of plasma oxTrp72-apoA1 and total apoA1 levels in the cohort revealed substantial variability among subjects. On average, only 0.007% of apoA1 in plasma harbored the 2-OH-Trp72 moiety (**Fig. 5g**). In contrast, oxTrp72-apoA1 represented 20% of total apoA1 within atherosclerotic plaque–laden aorta (n = 10) (**Fig. 5g** and **Supplementary Fig. 7a**,**b**), and is thus greater than 1,000-fold more abundant (relative to total apoA1) in plaque compared to plasma. For illustrative purposes, we also examined plasma from a random sampling of subjects from the cohort without (n = 8) or with (n = 8) CVD using SDS-PAGE and either Coomassie Blue staining for protein or western blot analyses using each of the mAbs used in the sandwich immunoassay (**Supplementary Fig. 7c–e**). Of note, both capture (mAb r8B5.2) and detection (mAb 10G1.5) antibodies in the ELISA recognized a single major band in plasma at the molecular weight of apoA1 monomer, although with overexposure, bands were also notable at molecular weights corresponding to apoA1 dimer and higher molecular weight oxidative cross-linked multimers.

Over the entire cohort, we observed the expected inverse correlations of HDLc and apoA1 levels with CAD and CVD (**Supplementary Fig. 7f–i**). In contrast, the absolute concentration of oxTrp72-apoA1 and the ratio of oxTrp72-apoA1 to total apoA1 was significantly higher in subjects with either CAD or CVD compared to their corresponding controls (i.e., non-CAD or non-CVD, respectively; **Fig. 5h**). Logistic regression models with adjustment for traditional cardiac risk factors (age, sex, hypertension, diabetes mellitus, current or former smoker, LDLc and HDLc), triglycerides, apoA1, high-sensitivity C-reactive protein, MPO, HbA1c and history of lipid-lowering medicine were used to estimate odds ratio and 95% confidence interval for CVD or CAD. Higher levels of circulating oxTrp72-apoA1 (both absolute concentration and as a ratio relative to total apoA1) were independently associated with increased CAD and CVD risk, particularly when comparing the fourth quartile to the first (**Fig. 5i** and **Supplementary Table 2b**). The positive associations with increased CAD or CVD risk remained significant even after adjustments for traditional CVD risk factors, apoA1, MPO and high sensitivity C-reactive protein levels, and the use of lipid-lowering medication (**Fig. 5i** and **Supplementary Table 2b**). We evaluated the improvement in logistic regression model (Online Methods) performance introduced by the inclusion of oxTrp72-apoA1 using the net reclassification index and the integrated discrimination improvement. Though there was no significant gain in the area under the curve (i.e., the receiver operating characteristic curve), inclusion of oxTrp72-apoA1 in the fully adjusted model resulted in a significant improvement in risk estimation based on the net reclassification index (CAD: 4.1%, $P < 0.001$; CVD: 5.9%, $P < 0.001$) and the integrated discrimination improvement (20% for both CAD and CVD, $P < 0.001$). Of note, the prognostic values of HDLc and apoA1 each demonstrated the expected inverse association with CVD and CAD risk (**Fig. 5i** and **Supplementary Table 2b**). We also performed comparisons of the odds ratios (and 95% confidence intervals) for oxTrp72-apoA1 plasma concentration versus traditional risk factors for CVD and found that the odds ratios observed using oxTrp72-apoA1 concentrations as a continuous variable were comparable in magnitude to numerous established risk factors within the cohort (**Supplementary Table 2c**).

DISCUSSION

The atheroprotective role of HDL has been questioned because of both recent failures of multiple HDLc-raising drugs and Mendelian randomization studies showing that genetic variants that control HDLc levels are not associated with risk of CAD[16–18,37]. Yet there is overwhelming preclinical data showing that apoA1 has anti-atherosclerotic effects[1,3,5,6]. This apparent contradiction has spurred interest in better understanding the role of the HDL particle in human CAD. Ideally, HDL in the circulation should be monitored in a manner that reflects its function within the artery wall. Studies thus far have shown that apoA1 recovered from human atheroma is highly oxidized, crosslinked, dysfunctional (with respect to cholesterol efflux and LCAT activities) and lipid poor, as it is not associated with an HDL particle[25]. Despite the recognition that apoA1 in lesions is heavily oxidized, direct functional interrogation of a structurally specific oxidative modification on apoA1 recovered from the artery wall has not been reported, to our knowledge. Our present studies identify the structural basis of an abundant dysfunctional form of apoA1 and HDL within the artery wall: MPO-catalyzed site-specific oxidation of Trp72 of apoA1 forming an oxindolyl alanine (2-OH-Trp) moiety. We found that this form of apoA1 is highly prevalent in human atheroma, accounting for one in five apoA1s within the lesion. Notably, the oxidized apoA1 form oxTrp72-apoA1 was minimally associated with HDL particles, with virtually all oxTrp72-apoA1 in both the artery wall and plasma recovered as a lipid-poor form. Thus, isolation of HDL-like particles recovered from human arterial lesion homogenates using buoyant density ultracentrifugation, an approach used by some researchers when studying apoA1 from lesions[38,39], misses the vast majority of this abundant modified form of apoA1 *in vivo*. We also found that lipid-free oxTrp72-apoA1 recovered from human plasma, like lipid-poor apoA1 modified by the MPO-H_2O_2-Cl^- system, is proinflammatory, capable of inducing endothelial cell NF-κB activation and nuclear localization, as well as surface expression of VCAM1 protein, an adhesion protein with known proatherogenic function[40]. Whether differences in lipid binding capability of oxidized as compared to native apoA1 forms contribute to pathophysiological functions is unclear.

An overall scheme of our findings is illustrated in **Figure 6a**. Circulating HDL readily diffuses into the artery wall. Within atherosclerotic lesions, MPO is enriched and promotes site-specific oxidative modification of apoA1 at residue Trp72. The results of site-directed mutagenesis studies show that this residue is essential for the ABCA1-dependent cholesterol efflux activity of apoA1 *in vitro*, and animal model studies with the 72WF-apoA1 mutant demonstrate the importance of this residue in loss of apoA1 association with HDL particles *in vivo* after MPO-catalyzed oxidation. Recovery of

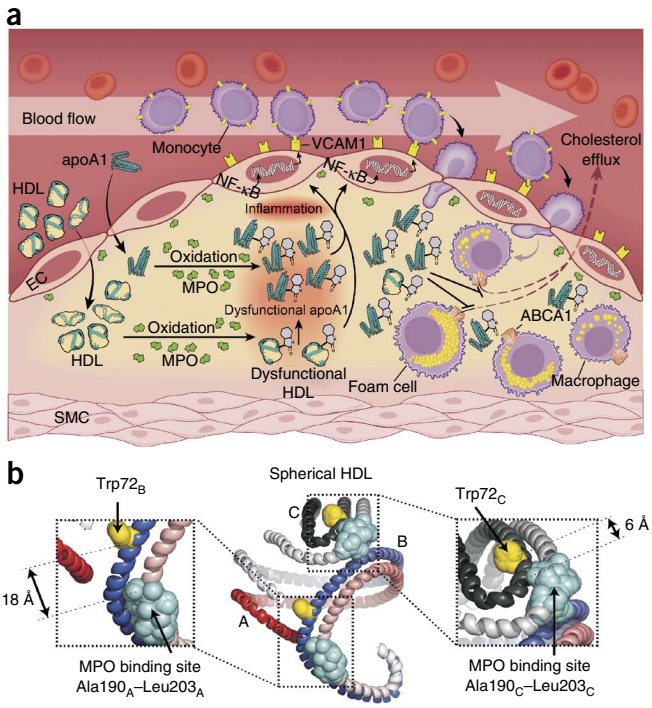

Figure 6 Formation of a dysfunctional apoA1 form, oxTrp72-apoA1, within human atherosclerotic lesions. (**a**) Schematic summary illustrating the formation of an abundant dysfunctional apoA1 form in human atheroma generated by MPO (see text for details). EC, endothelial cell; SMC, smooth muscle cell. (**b**) Model of spherical HDL demonstrating the close spatial proximity between the MPO binding site on one apoA1 chain and Trp72 on the contralateral anti-parallel apoA1 chain. There are three apoA1 chains in the reconstituted spherical HDL shown. Each chain has a Trp72 that is in close spatial proximity to an MPO binding site on a contralateral apoA1 chain (labels A, B and C indicate the general locations of oxTrp and corresponding closest MPO binding site). Shown are the longest (18 Å) and shortest (6 Å) predicted distances between oxTrp72 and the MPO binding site on the contralateral apoA1 among the three apoA1 chains[43]. The apoA1 polypeptide chains are depicted in red and slate gray. Trp72, yellow; MPO interaction site with apoA1, light blue.

apoA1 from lesions using a mAb specific for oxTrp72-apoA1 revealed virtually no detectable ABCA1-dependent cholesterol acceptor activity and potent proinflammatory activity. Notably, injection of apoA1 harboring the 2-OH-Trp moiety into apoA1 KO mice con-firmed that this apoA1 form is impaired in HDL biogenesis activity, as it failed to elicit an increase in circulating HDLc levels or appear on HDL particles.

The MPO-H_2O_2-Cl^- oxidative system generates a 2-oxindolyl alanine (2-OH-Trp) moiety on apoA1 at Trp72, and our detailed structural analyses reveal a remarkable specificity for both oxida-tion at Trp72 and on the indole ring at the 2 position. The selective targeting of the Trp72 site of apoA1 by the MPO system, but not by alternative oxidation systems, appears to have a structural basis: the close proximity between the MPO binding site on the antiparallel apoA1 chain and Trp72 of apoA1 (**Fig. 6b**). It is widely believed that apoA1 within HDL is configured predominantly as antiparallel amphipathic alpha-helical chains[27,41–45]. We recently used small-angle neutron scattering with contrast variation to directly visualize the protein shape of apoA1 within spherical HDL, the most abundant form of HDL in the circulation[44]. Coupled with crosslinking mass spectrometry studies and molecular modeling, we developed a model of apoA1 within spherical HDL[44]. In this model, the dis-tance between Trp72 and the MPO binding region on apoA1, which was identified by hydrogen-deuterium exchange (residues Ala190–Leu203)[26], is remarkably short, ranging between a maximum predicted length of 18 Å to a minimal distance of only 6 Å (**Fig. 6b**). Moreover, the predicted distance between Trp72 of one apoA1 chain and the MPO binding site on the adjacent apoA1 chain in nascent HDL shows a similarly short distance (14 Å) (**Supplementary Fig. 8**). The oxidant formed by the MPO-H_2O_2-Cl^- system, HOCl, is highly reactive and is scavenged rapidly by the first susceptible target it encounters (which is virtually any amino acid, though methionine, cysteine, histidine, tryptophan, lysine and tryosine are the most reactive[46]). In all structural models of HDL reported, the MPO binding site and Trp72 are separated by a short diffusion distance, which probably contributes to the selective targeting of Trp72 for oxidative modification by MPO (**Fig. 6b**).

Although oxTrp72-apoA1 is highly enriched within the athero-sclerotic plaque, no detectable immunostaining with mAb 8B5.2 was observed within normal aortic tissue. Thus, within the artery wall, MPO-dependent oxidative modification of apoA1 appears to be highly correlated with the atherosclerotic disease process. However, we did observe an increase in circulating oxTrp72-apoA1 levels in a mouse model of peritonitis. Thus, apoA1 may be oxidized at a local site of inflammation, whether the artery wall or an inflamed peritoneal cav-ity, and then diffuse into the circulation. Based on these results, we would not anticipate that oxTrp72-apoA1 levels in the circulation could serve as a specific indicator of atherosclerosis. Nonetheless, multilogistic regression analyses within the clinical cohort examined demonstrate that elevated levels of oxTrp72-apoA1 are associated with CAD and CVD risk, associations that remain statistically sig-nificant after adjustments for multiple traditional risk factors, includ-ing apoA1, MPO and other markers of inflammation. It is possible that the proinflammatory activity of oxTrp72-apoA1 may render it proatherogenic, such that elevated levels of oxTrp72-apoA1 may con-tribute to the well-recognized phenomenon of increased CVD risk during chronic inflammatory conditions. However, further studies are needed to test this intriguing hypothesis.

Our studies suggest that formation of oxTrp72-apoA1 occurs within the protected environment of the subendothelial space (**Fig. 6a**), and that this oxidized form of apoA1 then diffuses out of the artery wall to reach the intravascular compartment. MPO has been shown to accumulate within the subendothelial compartment[47] and has been mechanistically linked to the formation of vulnerable plaques by mechanisms including catalytic consumption of nitric oxide[48,49], activation of matrix metalloproteinase pathways[50] and promotion of endothelial cell apoptosis and superficial erosions within culprit lesions[51]. Indeed, MPO is currently being examined as a poten-tial target for functional imaging of vulnerable plaque[52,53] and as a pharmacological target for treatment of CVD. The present studies suggest that quantification of oxTrp72-apoA1 within the circulation may serve as a gauge of proatherosclerotic processes that impair apoA1 and HDL function in the artery wall and that oxTrp72-apoA1 may serve as a new diagnostic and therapeutic target in CAD.

METHODS

Methods and any associated references are available in the online version of the paper.

Note: Any Supplementary Information and Source Data files are available in the online version of the paper.

ACKNOWLEDGMENTS

We thank M. Liang (Chinese Center for Disease Control and Prevention) for the gift of the dicistronic baculoviral shuttle vector used to subclone the scFv gene. This study was supported by US National Institutes of Health (NIH) grants P01HL098055 and HL119962. BioBank, the clinical study from which samples were analyzed, was supported in part from NIH grants P01HL098055, P01HL076491, R01HL103866, P20HL113452 and R01HL103931. This work was also supported in part by a grant from the LeDucq Fondation. S.L.H. is also partially supported by a gift from the Leonard Krieger Fund. Mass spectrometry instrumentation used was housed within the Cleveland Clinic Mass Spectrometry Facility, which is partially supported through a Center of Innovation Award by AB SCIEX.

AUTHOR CONTRIBUTIONS

Y.H. participated in all laboratory, animal and human studies, assisted in statistical analyses, helped design the experiments and drafted the manuscript. B.S.L., G.S.G., V.G., C.S.K., Z.W. and X.F. assisted with various laboratory and mass spectrometry studies. D.S., J.B., M.K.C., S.Z.B. and C.-C.C. helped perform various animal experiments. J.A.D., D.S., T.K., X.G., M.K.C., J.E.H., A.J.D. and D.P. helped make various bacterial expression clones and produce and purify recombinant proteins used. J.A.D. and S.L. helped with mAb generation and screening. T.K. and T.T.N. helped with ELISA assays. L.L. and Y.W. provided statistical analyses of clinical data. J.A.D., L.C., E.F.P., P.L.F., V.G., W.H.W.T., J.S.P., E.A.F., J.D.S. and S.L.H. provided experimental analysis and expertise. All authors took part in critical review of the manuscript. The project was scientifically conceived and directed by S.L.H.

COMPETING FINANCIAL INTERESTS

The authors declare competing financial interests: details are available in the online version of the paper.

1. Barter, P.J. *et al.* Antiinflammatory properties of HDL. *Circ. Res.* **95**, 764–772 (2004).
2. Duffy, D. & Rader, D.J. Update on strategies to increase HDL quantity and function. *Nat. Rev. Cardiol.* **6**, 455–463 (2009).
3. Navab, M., Reddy, S.T., Van Lenten, B.J. & Fogelman, A.M. HDL and cardiovascular disease: atherogenic and atheroprotective mechanisms. *Nat. Rev. Cardiol.* **8**, 222–232 (2011).
4. Khera, A.V. *et al.* Cholesterol efflux capacity, high-density lipoprotein function, and atherosclerosis. *N. Engl. J. Med.* **364**, 127–135 (2011).
5. Vickers, K.C., Palmisano, B.T., Shoucri, B.M., Shamburek, R.D. & Remaley, A.T. MicroRNAs are transported in plasma and delivered to recipient cells by high-density lipoproteins. *Nat. Cell Biol.* **13**, 423–433 (2011).
6. Fisher, E.A., Feig, J.E., Hewing, B., Hazen, S.L. & Smith, J.D. High-density lipoprotein function, dysfunction, and reverse cholesterol transport. *Arterioscler. Thromb. Vasc. Biol.* **32**, 2813–2820 (2012).
7. Gordon, T., Castelli, W.P., Hjortland, M.C., Kannel, W.B. & Dawber, T.R. High density lipoprotein as a protective factor against coronary heart disease. The Framingham Study. *Am. J. Med.* **62**, 707–714 (1977).
8. Badimon, J.J., Badimon, L., Galvez, A., Dische, R. & Fuster, V. High density lipoprotein plasma fractions inhibit aortic fatty streaks in cholesterol-fed rabbits. *Lab. Invest.* **60**, 455–461 (1989).
9. Badimon, J.J., Badimon, L. & Fuster, V. Regression of atherosclerotic lesions by high density lipoprotein plasma fraction in the cholesterol-fed rabbit. *J. Clin. Invest.* **85**, 1234–1241 (1990).
10. Rubin, E.M., Krauss, R.M., Spangler, E.A., Verstuyft, J.G. & Clift, S.M. Inhibition of early atherogenesis in transgenic mice by human apolipoprotein AI. *Nature* **353**, 265–267 (1991).
11. Plump, A.S., Scott, C.J. & Breslow, J.L. Human apolipoprotein A-I gene expression increases high density lipoprotein and suppresses atherosclerosis in the apolipoprotein E–deficient mouse. *Proc. Natl. Acad. Sci. USA* **91**, 9607–9611 (1994).
12. Hughes, S.D., Verstuyft, J. & Rubin, E.M. HDL deficiency in genetically engineered mice requires elevated LDL to accelerate atherogenesis. *Arterioscler. Thromb. Vasc. Biol.* **17**, 1725–1729 (1997).
13. Nissen, S.E. *et al.* Effect of recombinant ApoA-I Milano on coronary atherosclerosis in patients with acute coronary syndromes: a randomized controlled trial. *J. Am. Med. Assoc.* **290**, 2292–2300 (2003).
14. Sacks, F.M. *et al.* Selective delipidation of plasma HDL enhances reverse cholesterol transport *in vivo*. *J. Lipid Res.* **50**, 894–907 (2009).
15. Tardif, J.C. *et al.* Effects of reconstituted high-density lipoprotein infusions on coronary atherosclerosis: a randomized controlled trial. *J. Am. Med. Assoc.* **297**, 1675–1682 (2007).
16. Barter, P.J. *et al.* Effects of torcetrapib in patients at high risk for coronary events. *N. Engl. J. Med.* **357**, 2109–2122 (2007).
17. Nissen, S.E. *et al.* Effect of torcetrapib on the progression of coronary atherosclerosis. *N. Engl. J. Med.* **356**, 1304–1316 (2007).
18. Boden, W.E. *et al.* Niacin in patients with low HDL cholesterol levels receiving intensive statin therapy. *N. Engl. J. Med.* **365**, 2255–2267 (2011).
19. Voight, B.F. *et al.* Plasma HDL cholesterol and risk of myocardial infarction: a mendelian randomisation study. *Lancet* **380**, 572–580 (2012).
20. Bhattacharyya, T. *et al.* Relationship of paraoxonase 1 (PON1) gene polymorphisms and functional activity with systemic oxidative stress and cardiovascular risk. *J. Am. Med. Assoc.* **299**, 1265–1276 (2008).
21. Besler, C. *et al.* Mechanisms underlying adverse effects of HDL on eNOS-activating pathways in patients with coronary artery disease. *J. Clin. Invest.* **121**, 2693–2708 (2011).
22. Sorci-Thomas, M.G. & Thomas, M.J. High density lipoprotein biogenesis, cholesterol efflux, and immune cell function. *Arterioscler. Thromb. Vasc. Biol.* **32**, 2561–2565 (2012).
23. Shih, D.M. *et al.* Combined serum paraoxonase knockout/apolipoprotein E knockout mice exhibit increased lipoprotein oxidation and atherosclerosis. *J. Biol. Chem.* **275**, 17527–17535 (2000).
24. Tang, W.H. *et al.* Clinical and genetic association of serum paraoxonase and arylesterase activities with cardiovascular risk. *Arterioscler. Thromb. Vasc. Biol.* **32**, 2803–2812 (2012).
25. DiDonato, J.A. *et al.* Function and distribution of apolipoprotein A1 in the artery wall are markedly distinct from those in plasma. *Circulation* **128**, 1644–1655 (2013).
26. Zheng, L. *et al.* Apolipoprotein A-I is a selective target for myeloperoxidase-catalyzed oxidation and functional impairment in subjects with cardiovascular disease. *J. Clin. Invest.* **114**, 529–541 (2004).
27. Wu, Z. *et al.* The refined structure of nascent HDL reveals a key functional domain for particle maturation and dysfunction. *Nat. Struct. Mol. Biol.* **14**, 861–868 (2007).
28. Peng, D.Q. *et al.* Apolipoprotein A-I tryptophan substitution leads to resistance to myeloperoxidase-mediated loss of function. *Arterioscler. Thromb. Vasc. Biol.* **28**, 2063–2070 (2008).
29. Undurti, A. *et al.* Modification of high density lipoprotein by myeloperoxidase generates a pro-inflammatory particle. *J. Biol. Chem.* **284**, 30825–30835 (2009).
30. Hadfield, K.A. *et al.* Myeloperoxidase-derived oxidants modify apolipoprotein A-I and generate dysfunctional high-density lipoproteins: comparison of hypothiocyanous acid (HOSCN) with hypochlorous acid (HOCl). *Biochem. J.* **449**, 531–542 (2013).
31. Van Lenten, B.J. *et al.* Anti-inflammatory HDL becomes pro-inflammatory during the acute phase response. Loss of protective effect of HDL against LDL oxidation in aortic wall cell cocultures. *J. Clin. Invest.* **96**, 2758–2767 (1995).
32. Ansell, B.J. *et al.* Inflammatory/antiinflammatory properties of high-density lipoprotein distinguish patients from control subjects better than high-density lipoprotein cholesterol levels and are favorably affected by simvastatin treatment. *Circulation* **108**, 2751–2756 (2003).
33. Charles-Schoeman, C. *et al.* Effects of high-dose atorvastatin on antiinflammatory properties of high density lipoprotein in patients with rheumatoid arthritis: a pilot study. *J. Rheumatol.* **34**, 1459–1464 (2007).
34. Shao, B., Pennathur, S. & Heinecke, J.W. Myeloperoxidase targets apolipoprotein A-I, the major high density lipoprotein protein, for site-specific oxidation in human atherosclerotic lesions. *J. Biol. Chem.* **287**, 6375–6386 (2012).
35. Brennan, M.L. *et al.* A tale of two controversies: defining both the role of peroxidases in nitrotyrosine formation *in vivo* using eosinophil peroxidase and myeloperoxidase-deficient mice, and the nature of peroxidase-generated reactive nitrogen species. *J. Biol. Chem.* **277**, 17415–17427 (2002).
36. Timmins, J.M. *et al.* Targeted inactivation of hepatic Abca1 causes profound hypoalphalipoproteinemia and kidney hypercatabolism of apoA-I. *J. Clin. Invest.* **115**, 1333–1342 (2005).
37. Barter, P.J. & Kastelein, J.J. Targeting cholesteryl ester transfer protein for the prevention and management of cardiovascular disease. *J. Am. Coll. Cardiol.* **47**, 492–499 (2006).
38. Bergt, C. *et al.* The myeloperoxidase product hypochlorous acid oxidizes HDL in the human artery wall and impairs ABCA1-dependent cholesterol transport. *Proc. Natl. Acad. Sci. USA* **101**, 13032–13037 (2004).
39. Shao, B. *et al.* Tyrosine 192 in apolipoprotein A-I is the major site of nitration and chlorination by myeloperoxidase, but only chlorination markedly impairs ABCA1-dependent cholesterol transport. *J. Biol. Chem.* **280**, 5983–5993 (2005).
40. Cybulsky, M.I. *et al.* A major role for VCAM-1, but not ICAM-1, in early atherosclerosis. *J. Clin. Invest.* **107**, 1255–1262 (2001).
41. Segrest, J.P. *et al.* A detailed molecular belt model for apolipoprotein A-I in discoidal high density lipoprotein. *J. Biol. Chem.* **274**, 31755–31758 (1999).
42. Wu, Z. *et al.* Double superhelix model of high density lipoprotein. *J. Biol. Chem.* **284**, 36605–36619 (2009).
43. Gogonea, V. *et al.* Congruency between biophysical data from multiple platforms and molecular dynamics simulation of the double-super helix model of nascent high-density lipoprotein. *Biochemistry* **49**, 7323–7343 (2010).
44. Wu, Z. *et al.* The low resolution structure of ApoA1 in spherical high density lipoprotein revealed by small angle neutron scattering. *J. Biol. Chem.* **286**, 12495–12508 (2011).

45. Gogonea, V. *et al.* The low-resolution structure of nHDL reconstituted with DMPC with and without cholesterol reveals a mechanism for particle expansion. *J. Lipid Res.* **54**, 966–983 (2013).
46. Pattison, D.I. & Davies, M.J. Absolute rate constants for the reaction of hypochlorous acid with protein side chains and peptide bonds. *Chem. Res. Toxicol.* **14**, 1453–1464 (2001).
47. Baldus, S. *et al.* Endothelial transcytosis of myeloperoxidase confers specificity to vascular ECM proteins as targets of tyrosine nitration. *J. Clin. Invest.* **108**, 1759–1770 (2001).
48. Abu-Soud, H.M. & Hazen, S.L. Nitric oxide is a physiological substrate for mammalian peroxidases. *J. Biol. Chem.* **275**, 37524–37532 (2000).
49. Eiserich, J.P. *et al.* Myeloperoxidase, a leukocyte-derived vascular NO oxidase. *Science* **296**, 2391–2394 (2002).
50. Wang, Y. *et al.* Myeloperoxidase inactivates TIMP-1 by oxidizing its N-terminal cysteine residue: an oxidative mechanism for regulating proteolysis during inflammation. *J. Biol. Chem.* **282**, 31826–31834 (2007).
51. Sugiyama, S. *et al.* Hypochlorous acid, a macrophage product, induces endothelial apoptosis and tissue factor expression: involvement of myeloperoxidase-mediated oxidant in plaque erosion and thrombogenesis. *Arterioscler. Thromb. Vasc. Biol.* **24**, 1309–1314 (2004).
52. Nahrendorf, M. *et al.* Activatable magnetic resonance imaging agent reports myeloper-oxidase activity in healing infarcts and noninvasively detects the antiinflammatory effects of atorvastatin on ischemia-reperfusion injury. *Circulation* **117**, 1153–1160 (2008).
53. Ronald, J.A. *et al.* Enzyme-sensitive magnetic resonance imaging targeting myeloperoxidase identifies active inflammation in experimental rabbit atherosclerotic plaques. *Circulation* **120**, 592–599 (2009).

ONLINE METHODS

Materials. Human MPO was isolated and characterized as described[54]. [^{3}H]cholesterol was obtained from Amersham Biosciences (Piscataway, NJ). L-[$^{13}C_6$]tyrosine, L-[$^{13}C_9$,$^{15}N_1$]tyrosine, [$^{13}C_6$,$^{15}N_1$]leucine, L-[$^{13}C_9$,$^{15}N_1$]-phenylalanine and L-[$^{13}C_5$,$^{15}N_1$]valine were purchased from Cambridge Isotope Laboratories Inc. (Andover, MA). A mouse immunoglobulin isotyping kit was obtained from GIBCO BRL (Life Technologies GmbH). Trypsin was from Promega (Madison, WI), and all cell lines were from the American Type Culture Collection (Rockville, MD). 5-hydroxy-L-tryptophan was purchased from MP Biomedicals (Solon, OH). 6-hydroxyindole and 7-hydroxyindole were purchased from Chem-Impex International Inc (Wood Dale, IL). All peptides were synthesized by the CS Bio Company, Inc. (Menlo Park, CA). All other reagents were obtained from Sigma-Aldrich (St. Louis, MO) unless otherwise specified.

General procedures. All study protocols were approved by the Institutional Review Board of the Cleveland Clinic, and all subjects gave written informed consent. All mouse studies were performed under protocols approved by the Institutional Animal Care and Use Committee at the Cleveland Clinic.

Circulating HDL and plasma-derived purified apoA1 were obtained from healthy volunteer donors as previously described[55]. Protein content was determined by the Markwell-modified Lowry protein assay[56] with BSA as the standard. Recombinant human apoA1 was generated in an *Escherichia coli* expression system and isolated by sequential column chromatographies as described[26,57]. Briefly, rh-apoA1 and mutants were expressed in *E. coli* strain BL21 (DE-3) pLysS. All mutations were made using the QuickChange Mutagenesis Kit (Stratagene, La Jolla, CA) and confirmed by DNA sequencing. 4WF and 4WL represent recombinant human apoA1 in which all tryptophans (residues 8, 50, 72 and 108) were converted to phenylalanine or leucine. W8L, W50L, W72L, W72F, W108F and W108L are recombinant human apoA1 mutants with the indicated single tryptophan mutation. 3MV is an apoA1 mutant in which all three methionines (at residues 86, 112 and 148) were mutated to valine. 7YF is an apoA1 mutant in which all seven tyrosines (at residues 18, 29, 100, 115, 166, 192 and 236) were converted to phenylalanine. Reconstituted nascent HDL was prepared using the modified sodium cholate dialysis method[58] at an initial molar ratio of 100:10:1 of POPC (1-palmitoyl-2-oleoyl-*sn*-glycero-3-phosphocholine):cholesterol:apoA1. To remove all endotoxin from purified recombinant apoA1, all mutants were lipidated (using POPC:apoA1, 100:1 mol:mol), forming nascent HDL, and then delipidated by organic solvent extraction for six consecutive rounds. Endotoxin levels in all recombinant apoA1 were confirmed to be nominal (<0.5 EU mg^{-1} ml^{-1} protein) by Limulus amoebocyte lysate assay (Charles River Laboratories, Wilmington, MA). The concentration of apoA1 mutants was determined by both their predicted extinction coefficient at 280 nm and amino acid composition analyses after HCl hydrolysis (in the pure form). The accuracy of the protein concentrations of isolated pure apoA1 mutants was determined by stable isotope dilution LC/MS/MS analyses on an AB SCIEX 5000 triple quadrupole mass spectrometer using synthetic L-[$^{13}C_9$,$^{15}N_1$]tyrosine, [$^{13}C_6$,$^{15}N_1$]leucine, L-[$^{13}C_9$,$^{15}N_1$]phenylalanine and L-[$^{13}C_5$,$^{15}N_1$]valine as internal standards and the predicted sequence of the mutant. The concentration of H_2O_2 was determined spectrophotometrically (ε_{240} = 39.4 M^{-1} cm^{-1}). HOCl was added as NaOCl to the buffered reaction mixtures. The concentration of NaOCl was determined spectrophotometrically (ε_{292} = 350 M^{-1} cm^{-1}). Peroxynitrite ($ONOO^-$) was quantified spectrophotometrically (ε_{302} = 1,670 M^{-1} cm^{-1}). Protein-bound ClTyr was quantified by stable isotope dilution LC/MS/MS analyses using synthetic 3-Cl[$^{13}C_6$]tyrosine and L-[$^{13}C_9$,$^{15}N_1$]tyrosine as internal standards on an AB SCIEX 5000 triple quadrupole mass spectrometer as described[26,35]. Monoclonal antibodies specific for apoA1 or MPO-modified apoA1 (exposed to the MPO H_2O_2 Cl^- or MPO H_2O_2 NO_2^- system; H_2O_2:apoA1 molar ratio of 5:1) were generated using hybridoma technology[59]. The cholesterol efflux (ABCA1-dependent and total) activity of apoA1 was determined as described[26]. Specifically, RAW264.7 cells (ATCC, Rockville, MD) were treated with 2 μg ml^{-1} of apoA1(**Fig. 2b**,**e**) or the amount of proteins indicated in **Figure 3f** for 6 h. Efflux to the cholesterol acceptor was calculated as described[26]. 2,3,-dioxindolyl alanine and 2-oxindoly lalanine were synthesized as described[60]. Western blot quantification was done using either ImageJ software (version 1.46, http://rsbweb.nih.gov/ij/index.html) or Image Studio software (version 2, LI-COR Biosciences, Lincoln, NB). The HDL-containing lipoprotein fraction ($d \leq 1.21$ g ml^{-1}) and LPD fractions ($d > 1.21$ g ml^{-1}) were recovered from plasma or tissue homogenate by sequential buoyant density ultracentrifugation using sucrose and D_2O to avoid the high ionic strength–associated alterations to the protein composition of lipoprotein particles observed with KBr use[61]. Mouse plasma (10–40 μl) was diluted to 500 μl with 1× PBS buffer (pH 7.0) and 887 μl of sucrose D_2O buffer (d = 1.325 g ml^{-1}; 0.1742 g K_2HPO_4, 0.1361 g KH_2PO_4, 0.8182 g NaCl, 111.1 g sucrose and 100 ml of D_2O). The fraction with density less than 1.21 g ml^{-1} was obtained after a 48-h ultracentrifugation at 40,000 r.p.m. at 20 °C (Beckman rotor 50.4Ti; 8 × 49 mm ultra-clear centrifuge tubes). The lipoprotein fraction ($d \leq 1.21$ g ml^{-1}) was recovered by slicing the upper 0.25 ml of the tube. HDL cholesterol–precipitating reagent (StanBIO Laboratory, 0599) was added to mouse plasma to precipitate LDL, and HDL cholesterol was quantified by stable isotope dilution gas chromatography mass spectrometry analyses[62].

Phage display and affinity maturation of the parental antibody. A single-chain (scFv) phage display library was constructed using the cDNA derived from the 8B5.2 hybridoma cell line using methods described by Barbas *et al.*[63]. The murine κ variable light chain families VK1 to VK17 and the variable heavy chain families VH1 to VH19 were amplified using 26 pairs of family-specific primers, and then the variable light chain and variable heavy chain sequences were 'stitched' together with a flexible linker (SSGGGGSGGGGGGSSRSS) using overlap PCR and cloned into the phagemid pCOMB3 as described[63]. Recombinant phages were prepared from the library with the helper phage M13K07 at a multiplicity of infection of ~10. The library was selected using immunotubes (Costar #3690) coated with 0.5 ml 25 μg ml^{-1} Cl.apoA1 (apoA1 exposed to the MPO H_2O_2 Cl^- system at a 10:1 molar ratio of H_2O_2 to apoA1) in 50 mM carbonate buffer, pH 9.6, overnight at 4 °C (ref. 64). The rescue-selection-plating cycle was repeated three times. For affinity maturation, another phage display scFv library was constructed by error-prone PCR followed by passaging the library in XL1-red mutator *E. coli* (Stratagene, La Jolla, CA) four times. Screening of scFv by dissociation rate constant (K_{off}) was performed using real-time biospecific interaction analysis based on surface plasmon resonance (SPR) in a Biacore 2000 (GE Healthcare Life Sciences, Piscataway, NJ). A third library was generated by introducing all combinations of mutant residues found in nine individual gain-of-function clones into variable regions of the scFv gene. The scFv gene was subcloned to a dicistronic baculoviral shuttle vector (a generous gift from M. Liang, China CDC) and then recloned into the mammalian expression vector pcDNA3.1$^{(+)}$ (Life Technologies, Carlsbad, CA., catalog no. V790-20), and the dicistronic alleles were expressed in DG44 CHO cells as a chimeric mouse-human IgG antibody.

SPR. In a Biacore flow cell, approximately 2,000 resonance units (RU) of Cl.apoA1 (5 μg ml^{-1}) in 10 mM sodium acetate, pH 4.5, were coupled to a CM5 sensor chip. Association and dissociation rates of the original 8B5.2 and recombinant affinity-matured antibody were measured under a continuous flow of 30 ml min^{-1} using a concentration range from 0.7 to 1,000 nM. The K_a1 and K_d1 values were calculated using BIAeveluation software, and sensorgrams were fitted by a bivalent model. The apparent K_D was calculated from the ratio of K_d1/K_a1.

Immunopurification of oxTrp72apoA1. Antibodies were covalently coupled to UltraLink Hydrazide resin (Pierce Chemical Co., Rockford, IL) for immunoaffinity isolation of native or oxidized forms of apoA1 from plasma. Before immune-affinity isolations of apoA1 forms, human albumin was first depleted from the plasma as follows. Human plasma was dialyzed in a binding buffer (20 mM MOPS, (MOPS: Chem-Impex International, catalog no. 00217) pH 7.0, and 100 mM NaCl) and diluted fourfold in the binding buffer before it was loaded onto a 500-ml column bed of Q Sepharose XL resin (GE Healthcare Life Sciences, Piscataway, NJ). Albumin-depleted plasma was collected as flow through (western blot analyses with various anti-apoA1 mAbs confirmed complete recovery of all apoA1 forms (data not shown)). This flow-through fraction was delipidated and, to more completely remove contaminating immunoglobulins during the immune-affinity isolation step, reduced and denatured with guanidine hydrochloride (3 M final, pH 7.8) and dithiothreitol (1 mM final). After the denatured

fraction was incubated for 1 h at room temperature, the protein was alkylated by the addition of iodoacetamide (2.5 mM final) and incubated for 1 h at room temperature in a foil-wrapped container. The denatured and alkylated fraction was dialyzed against 20 mM Tris-Cl and 150 mM NaCl, and oxTrp72-apoA1 was purified from this solution using a covalently coupled r8B5.2 affinity column. Total apoA1 was similarly purified using a covalently coupled chicken polyclonal IgY that recognizes total apoA1 (anti-HDL IgY microbead slurry; catalog no. A20088-G100; Genway Biotech, San Diego, CA).

Cell surface VCAM1 protein expression. Cell surface VCAM1 protein levels were determined in BAECs (bovine aortic endothelial cells, Lonza Walkersville, Walkersville, MD, catalog no. AC-6001T25). BAECs were starved in DMEM for 4 h and then incubated with 80 μg of protein per ml of HDL or 80 μg of protein per ml of HDL exposed to the MPO H2O2 Cl– system (Cl.HDL) or, where indicated, individual protein and plasma for 16 h. After one wash with PBS, the cells were fixed in 4% paraformaldehyde for 20 min and blocked in 0.5% casein in PBS with 0.02% NaN_3 for 4 h. Surface VCAM1 protein was determined using goat polyclonal anti-VCAM1 primary antibody (1:4,000, sc-1504, Santa Cruz Biotechnology, Santa Cruz, CA) with anti-goat IgG antibody conjugated with horseradish peroxidase (1:5,000, sc-2020, Santa Cruz Biotechnology, Santa Cruz, CA) as a secondary antibody, detection by SureBlue tetramethylbenzidine peroxidase substrate (KPL Inc., Gaithersburg, MD) and measuring absorbance at 450 nm on a 96-well plate reader (Spectramax 384 Plus, Molecular Devices, Sunnyvale, CA) after the addition of 1 M HCl to stop the reaction.

Confocal immunofluorescent analysis. BAECs (2×10^4 cells per well) were inoculated into Lab-Tek Chamber 16-well glass slides (Electron Microscopy Sciences, Hatfield, PA) for 16 h. The cells were treated with drugs (**Fig. 4f**), 80 μg ml^{-1} each at 37 °C for 20 min. The cells were then washed with PBS and fixed with 4% paraformaldehyde in PBS (15 min, room temperature), permeabilized by immersion in 0.5% Triton X-100 (10 min, room temperature), quenched with 100 mM glycine (10 min, room temperature) and blocked in 1% BSA and 10% normal goat serum in PBS, pH 7.0 (1 h at room temperature). Blocked cells were incubated sequentially with primary antibody to NF-κB p65 (Glu498) (3987, Cell Signaling Technology, Danvers, MA) diluted (100-fold) in blocking buffer (overnight, 4 °C) and secondary antibody goat anti-rabbit IgG-FITC (ab6717-1, Abcam, Cambridge, MA) diluted in blocking buffer (100:1, 1 h, room temperature). Coverslips were mounted onto glass slides using Vectashield DAPI mounting medium (Vector Laboratories Inc., Burlingame, CA). Images were viewed on a Leica DMRXE confocal microscope (Leica Microsystems Inc, Buffalo Grove, IL) using a 63× oil-immersion objective with a 1.40 numeric aperture. Confocal images were acquired using the Leica Confocal Software Version 2.61.

Immunochemistry staining of atherosclerotic plaques. Fresh human aortic tissue was obtained as discarded surgical material, both at time of organ harvest from transplant donors, and during valve and aortic arch ('elephant trunk') replacement surgery. Immunohistochemistry of atherosclerotic plaques and normal aorta was carried out on fresh-frozen sections. The anti-oxTrp72apoA1 antibody (r8B5.2 Fab) and polyclonal rabbit anti-human MPO (A0398, Dako North America, Inc., Carpinteria, CA) were used at a dilution of 1:400. Mouse normal IgG1 (X0931, Dako North America, Inc., Carpinteria, CA) (diluted 400:1) was used as the control for antibody staining. The staining procedure followed the protocol of the DakoCytomation Envision+ system HRP(AEC) (Dako North America, Inc., Carpinteria, CA).

Aortic tissue homogenization. At the time of harvest, all tissues were immediately rinsed in ice-cold PBS supplemented with 100 μM diethylenetriamine pentaacetic acid (DTPA) and frozen at −80 °C in argon-sparged buffer A (65 mM sodium phosphate, pH 7.4, 100 μM DTPA and 100 μM butylated hydroxytoluene) in gas-tight containers overlaid with argon, which were kept within larger argon-flushed sealed containers. At the time of use, samples sealed in gas-tight containers were placed in an ice and water bath. Immediately before being complete thawed, tissues were rinsed five times with ice-cold argon-sparged Ca^{2+} and Mg^{2+}-free PBS supplemented with 100 μM DTPA to remove any residual visible hemoglobin. The aorta segment was rapidly cleaned of fatty tissues and placed in a Petri dish containing ice-cold PBS. The adventitial layer and outer portion of the media were carefully peeled from the vessel to give a clean smooth aorta. The aorta was rinsed with ice-cold PBS three times and the wet weight of the aorta was determined. The tissue was then cut into small pieces (about 3 to 5 mm in diameter) in a Petri dish cover on ice. Tissue pieces were suspended in ice-cold Ca^{2+} and Mg^{2+}-free PBS containing a protease inhibitor cocktail. The protease cocktail PMSF (1 mM) and Sigma-Aldrich protease inhibitor cocktail (P8340) were included in all subsequent solutions used for lipoprotein isolation. Aortic tissue was homogenized on ice with a Polytron Tissue Homogenizer (Model PT 10/35, Brinkman Instruments Inc., Westbury, NY) for 1 min followed by five 30-s intervals in an ice and water bath. The homogenate was then centrifuged at 12,000*g* for 30 min. The pellet was discarded and the supernatant was stored on ice until use. HDL and LPD fractions were separated by ultracentrifugation using a sucrose and D2O protocol[61].

Indirect ELISA. Nunc MaxSorp ELISA plates (#446612, Thermo Fisher Scientific, Waltham, MA) were coated with the indicated purified native or oxidized protein (0.2 μg ml^{-1}) in carbonate and bicarbonate buffer, pH 9.6. Purified human apoA1, rh-apoA1 and mutant apoA1s were modified by the MPO H_2O_2 Cl^- system, the MPO H_2O_2 NO_2^- system or multiple other oxidation systems, as indicated, at a 10:1 molar ratio of oxidants and apoA1, unless otherwise specified (the details of the oxidation conditions are described in ref. 25). The primary antibody r8B5.2 (50 ng ml^{-1}) (**Figs. 1d** and **2a**,**e**) was added into the 5% BSA–blocked ELISA wells and incubated for 1 h at room temperature. The plates were then washed with PBS and 0.05% Tween 20 (PBST) four times. Signal was detected by Peroxidase AffiniPure Goat Anti-Mouse IgG, F(ab′)2 Fragment Specific (1:10,000, code 115-036-006, Jackson ImmunoResearch Laboratories, Inc., West Grove, PA).

Competitive ELISA. Nunc MaxSorp ELISA plates (#446612, Thermo Fisher Scientific, Waltham, MA) were coated with 0.5 μg ml^{-1} Cl.apoA1 in carbonate and biocarbonate buffer, pH 9.6 (human apoA1 modified by the MPO H_2O_2 Cl^- complete oxidative system at a 10:1 molar ratio of H_2O_2 and apoA1). r8B5.2 (25 ng ml^{-1}) and peptides were added into the 5% BSA–blocked ELISA wells and incubated for 1 h at room temperature. The signal was detected by Peroxidase AffiniPure Goat Anti-Mouse IgG, F(ab′)2 Fragment Specific (1:10,000, code 115-036-006, Jackson ImmunoResearch Laboratories, Inc., West Grove, PA).

Sandwich ELISA. Costar ELISA plates (#3690) were coated with capture antibody r8B5.2 (50 μl per well, 7 μg ml^{-1} in 0.1 M Tris-Cl, pH 8.5) at 4 °C overnight. Except for the capture antibody coating process, all other reactions were performed at room temperature (20 °C). Coated plates were washed with PBS buffer twice, and then washed plates were blocked with 170 μl of blocking buffer (1% fish peptone (Fluka Biochemika, 93490), 3% BSA (Sigma, A7030), 2% poly vinyl alcohol and 0.05% Tween 20 in PBS, pH 7.4) for 2 h. A calibration curve was constructed with Cl.apoA1 (8 pM to 8 nM) in sample dilution buffer (1% salmon serum and 0.05% Tween 20 in PBS, pH 7.4). Pooled plasma samples that had been aliquoted into single-use samples were thawed once and used as controls on every plate. Plasma samples were diluted in sample dilution buffer (1% salmon serum and 0.05% Tween 20 in PBS, pH 7.4). Diluted samples were added into the blocked EIA wells at 50 μl per well and incubated for 45 min. The plates were then washed with PBST four times. The detection mAb 10G1.5 (anti-total apoA1[25]) was diluted (1:40,000) in antibody dilution buffer (0.03% BSA (Sigma, A7030) in PBST) and incubated in an EIA well at 50 μl per well for 30 min. After four washes with PBST, horseradish peroxidase–conjugated neutravidin (31001, Pierce Chemical Co., Rockford, IL; 1:10,000 diluted in antibody dilution buffer) was added into the ELISA plates (50 μl per well) and incubated for 30 min. The ELISA was developed with SureBlue TMB substrate (#52-00-0, KPL, Gaithersburg, MD) and the OD_{450} was determined.

Research subjects. Multiple healthy volunteers donated blood for isolation of apoA1, HDL, MPO and other human-derived plasma proteins used throughout the course of these studies. To examine the relationship between levels of oxTrp72-apoA1 and prevalence of CAD and CVD, a cohort of sequential consenting subjects ($n = 627$) presenting to the preventive cardiology outpatient clinic of the Cleveland Clinic was examined as part of an observational study called BioBank. Fasting plasma samples and associated clinical data were

collected at time of patient visit. The CAD definition included adjudicated diagnoses of stable or unstable angina, myocardial infarction, angiographic evidence of >50% stenosis of one or more major epicardial vessels or history of coronary revascularization. Peripheral artery disease (PAD) was defined as any evidence of extracoronary atherosclerosis or ankle brachial index <0.9. Atherosclerotic CVD was defined as the presence of either CAD or PAD. Patients who had experienced a myocardial infarction or stroke within the 1 month preceding enrollment were ineligible.

Mouse models. Breeders of all conventional mice C57BL/6 (catalog no. 000664), apoA1 homozygous transgenic (catalog no. 001927, C57BL/6-Tg(APOA1)1Rub/J) and ApoA1$^{-/-}$ mice (B6.129P2-*Apoa1*^{tm1Unc}, catalog no. 002055) were obtained from Jackson Laboratories. Control mice have a floxed ABCA1 gene (*Abca1*$^{flox/flox}$). Hepatocyte-specific ABCA1 knockout (*Abca1*$^{-L/-L}$; *Alb*-Cre) *Apoa1*$^{-/-}$ mice on a C57BL/6 background have been described[36,65]. In our previous study[36], we documented that wild-type ($^{+/+}$) and *Abca1*$^{flox/flox}$ mice have a similar plasma lipid phenotype. For the subacute peritonitis model, apoA1 homozygous transgenic animals were injected i.p. with zymosan. Plasma was obtained at baseline before injection and then serially (1, 2 and 3 d) after injection. OxTrp72-apoA1 levels in plasma were measured by sandwich ELISA using mAb r8B5.2 as the capture antibody and mAb 10G1.5 (anti-total apoA1[25]) as the detection antibody. To examine the role of hepatocyte ABCA1 in de novo HDL biogenesis *in vivo* after apoA1 injection, control mice (*Abca1*$^{flox/flox}$) and hepatocyte-specific ABCA1 KO mice (6–7 weeks old) (*Abca1*$^{-L/-L}$; *Alb*-Cre) were injected with the indicated form of apoA1 s.c. at 400 mg per kg body weight. Blood was collected by saphenous vein puncture 1 week before apoA1 injection (baseline) and 0.5 h, 1 h, 1.5 h and 2 h after apoA1 injection. ApoA1 KO mice were similarly injected s.c. with the indicated form of apoA1 at 400 mg per kg body weight, and the appearance and distribution of total human apoA1 and oxTrp72-apoA1 levels in the blood were monitored both at baseline and 2 h after apoA1 injection. All experiments were performed with female mice.

Statistical analyses. Data are presented as the median (first quartile–third quartile) for continuous measures and as a number (percentage) for categorical measures. Student's *t* test or Wilcoxon rank-sum test for continuous variables and χ^2 test for categorical variables were used to examine the differences between participants who had cardiovascular disease events and those who did not. Logistic regression models with adjustment for traditional Framingham cardiac risk factors (age, sex, hypertension, diabetes mellitus, current or former smoker, LDLc and HDLc), triglycerides, apoA1, high sensitivity C-reactive protein, MPO, HgbA1c and history of lipid-lowering medicine were used to estimate odds ratio and 95% confidence interval for CVD or CAD. All analyses were performed using R 2.15.0 (Vienna, Austria), and $P < 0.05$ was considered statistically significant.

54. Hazen, S.L. & Heinecke, J.W. 3-chlorotyrosine, a specific marker of myeloperoxidase-catalyzed oxidation, is markedly elevated in low density lipoprotein isolated from human atherosclerotic intima. *J. Clin. Invest.* **99**, 2075–2081 (1997).
55. Zamanian-Daryoush, M. *et al.* The cardioprotective protein apolipoprotein A1 promotes potent anti-tumorigenic effects. *J. Biol. Chem.* **288**, 21237–21252 (2013).
56. Markwell, M.A., Haas, S.M., Bieber, L.L. & Tolbert, N.E. A modification of the Lowry procedure to simplify protein determination in membrane and lipoprotein samples. *Anal. Biochem.* **87**, 206–210 (1978).
57. Ryan, R.O., Forte, T.M. & Oda, M.N. Optimized bacterial expression of human apolipoprotein A-I. *Protein Expr. Purif.* **27**, 98–103 (2003).
58. Matz, C.E. & Jonas, A. Micellar complexes of human apolipoprotein A-I with phosphatidylcholines and cholesterol prepared from cholate-lipid dispersions. *J. Biol. Chem.* **257**, 4535–4540 (1982).
59. Köhler, G. & Milstein, C. Continuous cultures of fused cells secreting antibody of predefined specificity. *Nature* **256**, 495–497 (1975).
60. Todorovski, T., Fedorova, M., Hennig, L. & Hoffmann, R. Synthesis of peptides containing 5-hydroxytryptophan, oxindolylalanine, N-formylkynurenine and kynurenine. *J. Pept. Sci.* **17**, 256–262 (2011).
61. Ståhlman, M. *et al.* Proteomics and lipids of lipoproteins isolated at low salt concentrations in D2O/sucrose or in KBr. *J. Lipid Res.* **49**, 481–490 (2008).
62. Robinet, P., Wang, Z., Hazen, S.L. & Smith, J.D. A simple and sensitive enzymatic method for cholesterol quantification in macrophages and foam cells. *J. Lipid Res.* **51**, 3364–3369 (2010).
63. Barbas, C.F. III, Burton, D.R., Scott, J.K. & Silverman, G.J. *Phage Display: A Laboratory Manual* (Cold Spring Harbor Laboratory Press, Cold Spring Harbor, New York, 2001).
64. Marks, J.D. *et al.* By-passing immunization. Human antibodies from V-gene libraries displayed on phage. *J. Mol. Biol.* **222**, 581–597 (1991).
65. Chung, S. *et al.* Targeted deletion of hepatocyte ABCA1 leads to very low density lipoprotein triglyceride overproduction and low density lipoprotein hypercatabolism. *J. Biol. Chem.* **285**, 12197–12209 (2010).